Structural and Hydrothermal Alteration Evidence for Early and Late Stages of Gold Mineralisation at the New Celebration gold deposits in Western Australia

S.J. Nichols, S.G. Hagemann and P. Neumayr
Centre for Global Metallogeny
School of Earth and Geographical Sciences
The University of Western Australia
Crawley, WA 6009

The New Celebration gold deposits (~2Moz Au) are located within the Boulder segment of the transcrustal (regional) Boulder-Lefroy fault zone about 35km southeast of Kalgoorlie, in the Kalgoorlie Terrane of the Eastern Goldfields Province, Western Australia. The gold deposits are hosted within ultramafic rocks (komatiite), differentiated gabbro/dolerite and thin (<5m wide) felsic porphyry dykes that have intruded the ultramafic-mafic rock contact. Host rocks have undergone regional metamorphism to upper greenschist facies.

Four deformation events are recorded at the New Celebration deposits: (1) D_{2NC} is represented by vertical stratigraphic contacts, the expression of upright folds formed on a regional scale in the New Celebration area. (2) D_{3NC} deformation is expressed as a well-developed, north-northwest trending, steeply west-southwest dipping penetrative shear foliation (S_{3NC}), which is representative of the regional D_3 Boulder fault zone. Lineations formed during D_{3NC} deformation include: (a) moderate to steep, south-southeast to south-southwest plunging L_{3mNC} mineral elongation lineations, (b) moderate, northwest plunging L_{3iNC} intersection lineations between S- and C-foliation planes, and (c) moderate to steep, south-southeast to south-southwest plunging L_{3sNC} slickenline lineations. Moderate to steep south-southwest plunging quartz L_{3mNC} elongation lineations, in conjunction with the orientation of S-C fabrics, constrain the sense of movement on the shear zone as sinistral oblique-slip, west-block-down to the south-southeast. The S_{3NC} foliation is also developed in thin (1 to 5m width) M_1 plagioclase-rich porphyry dykes thus indicating their formation pre- to syn-D_{3NC} deformation. The M_1 porphyry dykes are subsequently overprinted by the intrusion of second generation M_2 quartz-feldspar porphyry dykes, preferentially along the mafic-ultramafic rock contact. The lack of internal ductile deformation fabrics and a predominance of brittle structures (e.g., fractures) in M_2 porphyry dykes indicate their emplacement into a brittle deformation environment. (3) D_{4NC} deformation resulted in north-northeast trending, west-northwest dipping faults, quartz-carbonate vein sets and widely-spaced S_{4NC} foliation. Sub-horizontal L_{4sNC} slickenline lineations on D_{4NC} faults planes indicate strike-slip movement during D_{4NC} (no kinematic indicators observed). (4) D_{4+nNC} deformation represented by west-dipping curviplanar faults. Based on the markedly different orientations of D_{4+nNC} faults to D_{4NC} structures, curviplanar faults are interpreted to represent post-D_{4NC} deformation, although no cross cutting relationships are observed with D_{4NC} structures.

Two gold events are recognised at the New Celebration deposits: (1) an ‘early’ gold event in porphyry dykes (quartz-biotite-sericite-ankerite schists) is interpreted to be synchronous with the D_{3NC} deformation. Minute inclusions of gold (<100 microns) are hosted within pyrite that is aligned parallel to the S_{3NC} foliation planes. Gold occurs in equilibrium with sericite-ankerite-biotite and is also associated with gold

and non-gold bearing tellurides such as calerverite ($AuTe_2$), petzite (Ag_3AuTe_2), hessite (Ag_2Te), altaite (PbTe), melonite ($NiTe_2$) and a bismuth telluride; (2) a 'late' gold event within brittle fracture networks formed at the margins of the M_2 quartz-feldspar porphyry and adjacent high-magnesium basalt is interpreted to be synchronous to the D_{4NC} deformation event. In M_2 porphyry dykes 'free' gold and inclusions of gold in pyrite occur in equilibrium with sericite-ankerite-quartz±chlorite, whereas gold hosted in the high-magnesium basalt occurs in equilibrium with ankerite-sericite-quartz. No telluride species are observed associated with this gold mineralisation event.

The structurally controlled New Celebration gold deposits provide evidence for two stages of gold mineralization during D_{3NC} and D_{4NC} deformation events. 'Early' gold mineralization, emplaced in a ductile environment, is controlled by strain heterogeneity between M_1 porphyry dykes and D_3 ductile shear zones. 'Late' gold mineralization, located in a brittle environment, is controlled by the M_2 porphyry dykes and their contact with mafic and ultramafic rocks. Although geochronological data is presently not available, the contrast between ductile and brittle ore textures may suggest substantial uplift between the two gold stages. Significant amounts of tellurides in equilibrium with gold in the 'Early' gold event may point to a component of magmatic hydrothermal fluids circulating through the D_{3NC} shear zones.

KEY WORDS: alteration, Archaean, gold, Kalgoorlie, mineralisation, porphyry, structure, tellurium

INTRODUCTION

Structurally controlled Archaean gold deposits show a strong spatial relationship to first-order (>100km long) crustal-scale structures although are generally hosted within second- and third-order structures interpreted to be genetically related to first-order structures (Eisenlohr et al., 1989; Phillips et al., 1996; Neumayr et al., 2003). For example, the Golden Mile gold deposit (about 70 Million oz Au produced), about 30km north of New Celebration, is located within complex fault zones that are spatially related to the Boulder segment of the craton-scale Boulder-Lefroy fault zone (Phillips et al., 1996). Another example is the St. Ives gold camp, located approximately 20km south of the New Celebration gold deposits, which contains about 12 mines (10 Million oz Au produced) that are located in subsidiary structures west of the Boulder-Lefroy fault zone (Neumayr et al., 2003). Typically in the Yilgarn craton in Western Australia or the Superior Province in Canada, first-order structures, or transcrustal fault zones, rarely contain significant (>1 Million oz Au) orogenic gold deposits (Eisenlohr et al., 1989). Exception to this are the Kerr Addison deposit (5 Moz Au) in Canada (Kishida and Kerrich, 1987), the Paddington deposit (3 Moz Au) and the New Celebration gold deposits (2 Moz Au) of Western Australia (Nichols, 2003).

Therefore, the New Celebration gold deposits provide an ideal opportunity to investigate the structural controls, hydrothermal alteration and timing of gold mineralisation in a structurally complex segment of the first-order, transcrustal Boulder fault zone. Regional structural investigations by Swager et al. (1995) and Weinberg et al. (2003) concluded that the Boulder-Lefroy fault zone is a long-lived structure that formed early in the recognised regional deformation history and that it was most likely re-activated during subsequent D_3 and D_4 regional deformation events. The key question with regard to gold mineralisation pertains to its relative timing with respect to regional deformation, metamorphism and magmatism. For example, is gold introduced late during the sequence of regional deformation events, D4, as postulated for

the Kambalda-Kalgoorlie area (e.g. Swager et al., 1995; Witt et al., 1997) and for Archaean lode-gold deposits in the Yilgarn craton (Groves et al., 2000; Hagemann and Cassidy, 2000; Goldfarb et al., 2001), or is gold introduced during multiple deformation and gold mineralisation events as recently proposed in a new model for the giant Golden Mile deposit (Bateman et al., 2001; Bateman and Hagemann 2004).

The aim of this paper is to illustrate that gold mineralisation at New Celebration is structurally controlled by the Boulder segment of the transcrustal Boulder-Lefroy fault zone and that gold mineralisation styles identified at New Celebration represent two distinct structurally controlled gold mineralisation events ('Early' and 'Late' gold mineralisation) that differ in relative timing and are directly related to $D_{3regional}$ and $D_{4regional}$ deformation events. The first part of the paper describes the regional setting and structural evolution of the Boulder fault zone near New Celebration; the second part illustrates the orebody geometry and mineralisation styles, including hydrothermal alteration zonation. The third and final part provides an integrated structural-hydrothermal alteration model for the formation of the New Celebration gold deposits.

GEOLOGICAL SETTING

Regional Geology

The New Celebration gold deposits: Celebration, Mutooroo, Hampton Boulder Jubilee and Golden Hope are located about 35km southeast of Kalgoorlie, in the Kalgoorlie Terrane of the Eastern Goldfields Province, Western Australia (Figure 1). The Kalgoorlie Terrane is a regionally extensive area bounded to the west by the Ida fault and flanked to the east by the Mt Monger and Moraity shear zones (Swager et al., 1995; Swager, 1997).

The regional stratigraphic succession of the Kalgoorlie Terrane comprises a sequence of mafic-ultramafic lavas overlain by a felsic volcano-sedimentary unit which is in turn overlain by alluvial and fluviatile sedimentary rocks (Swager et al., 1995; Swager, 1997; Krapez et al., 2000). Differentiated basalt forms the lowermost unit of the stratigraphic sequence, with a minimum age of 2692$\pm$4 Ma, established from SHRIMP U-Pb zircon dating of a shale marker bed overlying the lower basalt unit (Swager, 1997). The basalt is overlain by a sequence of komatiite flows and thin, discontinuous sedimentary rock units; SHRIMP U-Pb zircon dating of shale marker beds defining the top of the komatiite unit constrains the minimum age of this unit to 2692$\pm$4 Ma (Swager, 1997). An upper basalt unit overlies the komatiite unit and is only observed in the Kambalda and Ora Banda Domains of the Kalgoorlie Terrane (Swager, 1997). The mafic and ultramafic rocks are overlain by a felsic volcano-sedimentary unit described by Krapez et al. (2000) as the Kalgoorlie Sequence. This unit comprises felsic volcanic rocks of rhyolitic to andesitic composition, quartzo-feldspathic siltstones, oligomictic and polymictic conglomerates and was deposited in two tectonic stages, with ages of 2681-2670 Ma and 2661-2655 Ma, for the first and second tectonic stage, respectively (SHRIMP U-Pb zircon dating; Krapez et al., 2000). Alluvial and fluviatile sedimentary rocks unconformably overlie the Kalgoorlie Sequence and have been dated using U-Pb zircon dating at 2655 Ma (Krapez et al., 2000).

The deformation history in the Kalgoorlie Terrane, summarised in Table 1, comprises four compressional events, D_1 – D_4, each preceded by episodes of extension. Early D_{1e} extension occurred in a north-south direction and was accompanied by plutonic magmatism between 2685-2675 Ma (Williams and Currie, 1993; Nelson, 1997). The D_1 compressive deformation event resulted in the formation of regional recumbent folds and thrust sheets (Swager, 1997; Weinberg et al., 2003) which was overprinted by regional

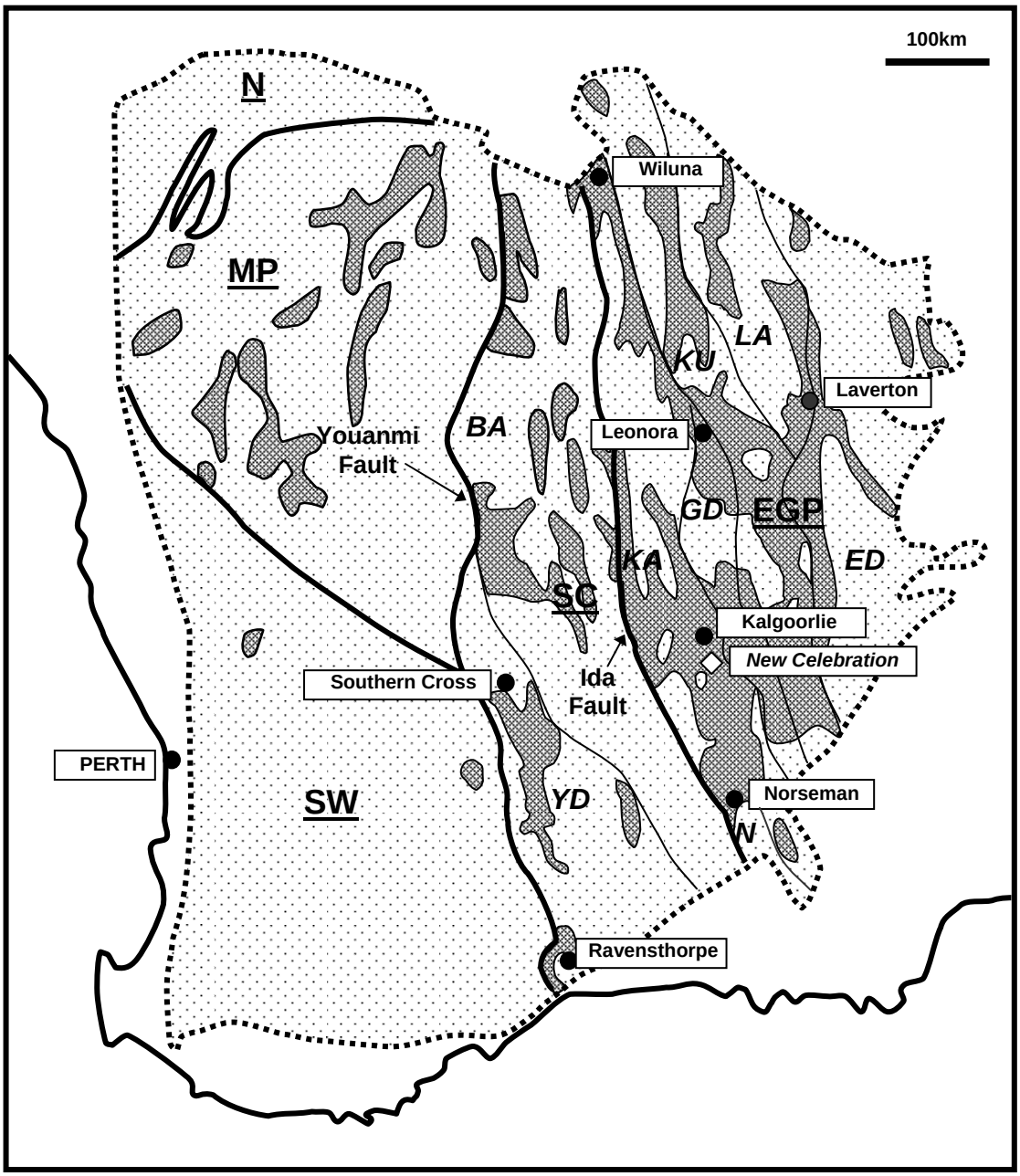

LEGEND

- Granite/Gneiss
- Greenstone
- Province Boundary Fault
- Terrane Boundary Fault
- Margin of Yilgarn Craton
- City or Town

Figure 1A: Map showing the position of provinces and terranes with respect to greenstone belts and granitoids of the Yilgarn Craton, Western Australia and the location of New Celebration approximately 35km southeast of the city of Kalgoorlie (Modified after Krapez et al., 2000).

Provinces: N = Narryer Province; MP = Murchison Province; SC = Southern Cross Province; EGP = Eastern Goldfields Province; SW = Southwestern Province

Terranes: YD = Yellowdine Terrane; BA = Barlee Terrane; KA = Kalgoorlie Terrane; N = Norseman Terrane; GD = Gindalbie Terrane; KU = Kurnalpie Terrane; LA = Laverton Terrane; ED = Edjudina Terrane

post-D_1 extension, D_{2e}, expressed as extensional basins developed on top of D_1 structures (Swager, 1997). The regional compressive D_2 event produced north-northwest trending upright folds and post-dated a voluminous felsic intrusive event spanning 2670-2655 Ma (Weinberg et al., 2003). The D_3 was a transpressive deformation event associated with the formation of north-northwest trending, sinistral, ductile shear zones (Weinberg et al., 2003), an example of which is the Boulder-Lefroy fault zone. The regional D_4 compressive deformation event resulted in north-northeast trending brittle shear or fault zones (Weinberg et al., 2003).

Regional metamorphic grades range from lower-greenschist facies to lower-amphibolite facies in the northern and southern parts of the Kalgoorlie Terrane, respectively, with peak regional metamorphic conditions suggested to have occurred late in the regional D_2 deformation event (Swager et al., 1995; Swager 1997; Archibald et al., 1978).

New Celebration Lithostratigraphy

The host rocks of the New Celebration gold deposits include ultramafic and differentiated mafic rocks juxtaposed by the Boulder segment of the north-northwest trending Boulder-Lefroy fault zone (henceforth Boulder fault zone). East of the Boulder fault zone the succession youngs eastward, whereas west of the fault zone the rock units are west younging (Archibald, 1992; Langsford, 1989). Two main generations of felsic intrusive rocks (M_1 plagioclase-rich porphyry dykes and M_2 quartz-feldspar porphyry dykes) also host gold and have intruded the mafic-ultramafic sequence sub-parallel to the sheared contact. With the exception of post-D_1 intrusive rocks, all of the rock units at New Celebration have undergone regional metamorphism to greenschist facies; for ease of reading the prefix meta- has been omitted henceforth.

Ultramafic rocks occur in the eastern footwall of the Hampton Boulder Jubilee open pit and the western wall of the Jubilee West pit (Figure 2). Commonly this rock is fine-grained (<0.05mm), homogeneous and equigranular in texture (Copeland et al., 1998) and displays a well-developed schistose foliation defined by the alignment of talc, although relict primary spinifex and cumulate textures are preserved in low strain zones (Figure 3A) pseudomorphed by metamorphic talc and hydrothermal magnetite (Figure 3B). Primary igneous minerals have been completely destroyed and replaced by serpentine, tremolite, chlorite, talc (Copeland et al., 1998; Norris, 1990; Langsford, 1989). The thickness of this unit is approximately 200m although the basal contact is not observed at New Celebration (Langsford, 1989).

A strongly differentiated mafic unit forms the hanging wall at Hampton Boulder Jubilee (Norris, 1990) and also forms the Eastern Domain at Jubilee West and Celebration (Figure 3C and 3D) (Archibald, 1992; Vearncombe, 1989). The mafic unit has been described in detail by Archibald (1992) and Langsford (1989) and comprises six main sub-units: (1) cumulative pyroxenite, (2) melanocratic dolerite containing elongate pyroxene blastophenocrysts up to 2cm in length in a fine grained groundmass of plagioclase, (3) equigranular magnetite-rich dolerite, (4) magnetite granophyre, 5) fine-grained oxide-rich dolerite containing bladed pyroxene phenocrysts, and (6) a fine-grained chilled zone. This mafic unit ranges in thickness from 200m – 600m (Langsford, 1989).

Two generations of porphyry dykes are recognised on the basis of relative cross cutting relationships and the timing within the structural evolution of the deposit. Early porphyry dykes attributed to the first magmatic event are designated M1, whereas late porphyry dykes, designated M_2, cross-cut and intrude M1

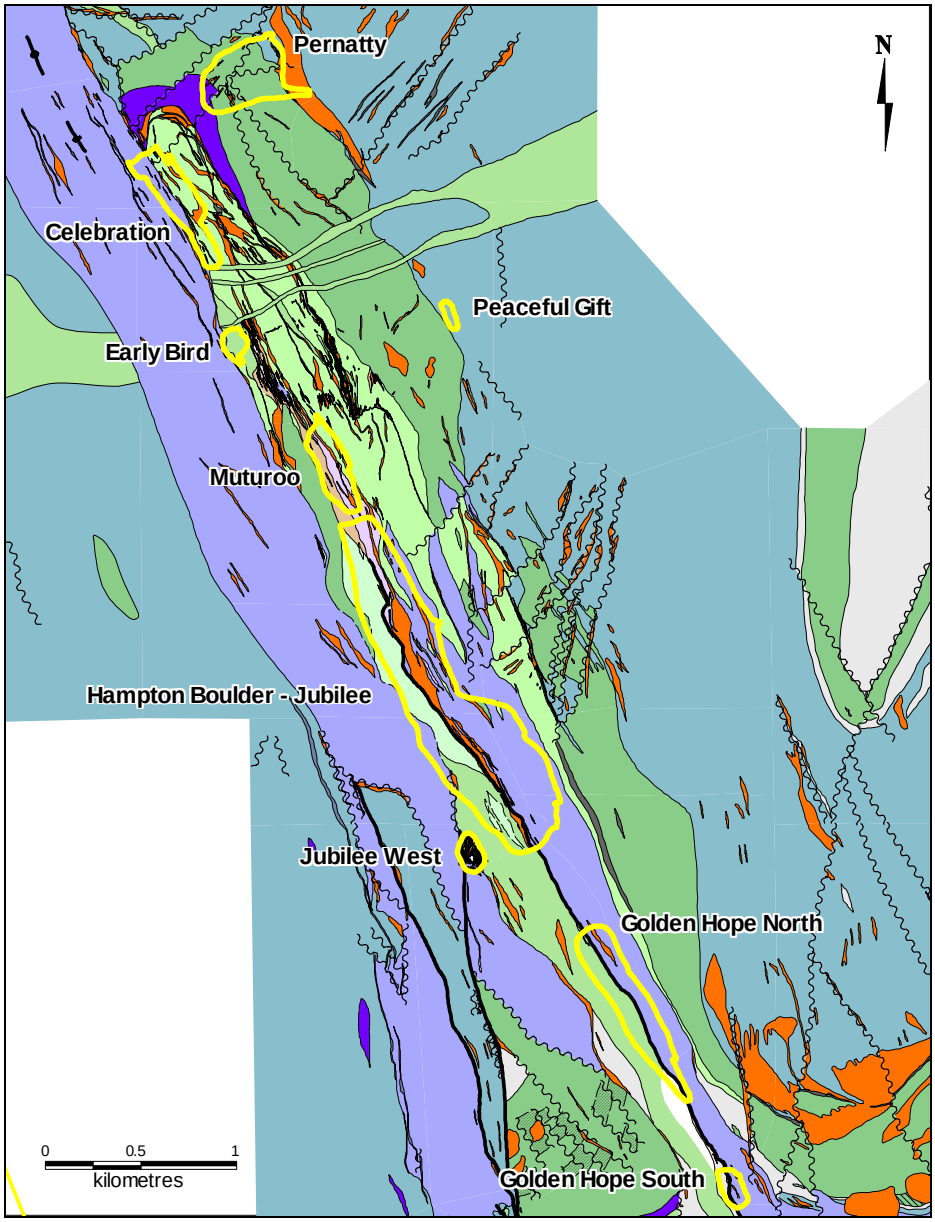

Lithological Legend

- Proterozoic Dyke
- Felsic Porphyry Dyke
- Black Shale
- Chert
- Felsic Volcaniclastic Sedimentary Rocks
- Mafic (Chlorite-Biotite) Schist
- Basalt
- Dolerite
- Gabbro
- High-Magnesium Basalt
- Pyroxenite
- Ultramafic (Talc-Carbonate-Chlorite) Schist
- Utlramafic

Figure 2A: Local geology of the New Celebration area showing the location of the New Celebration gold deposits parallel to the strike of the Boulder fault zone. The location of the Boulder fault zone and subsidiary structures interpretation is based on extensive field mapping and drill hole logging completed by South Kal Mines' geologists. This figure is published with the permission of Harmony South Kal Mines P.L.

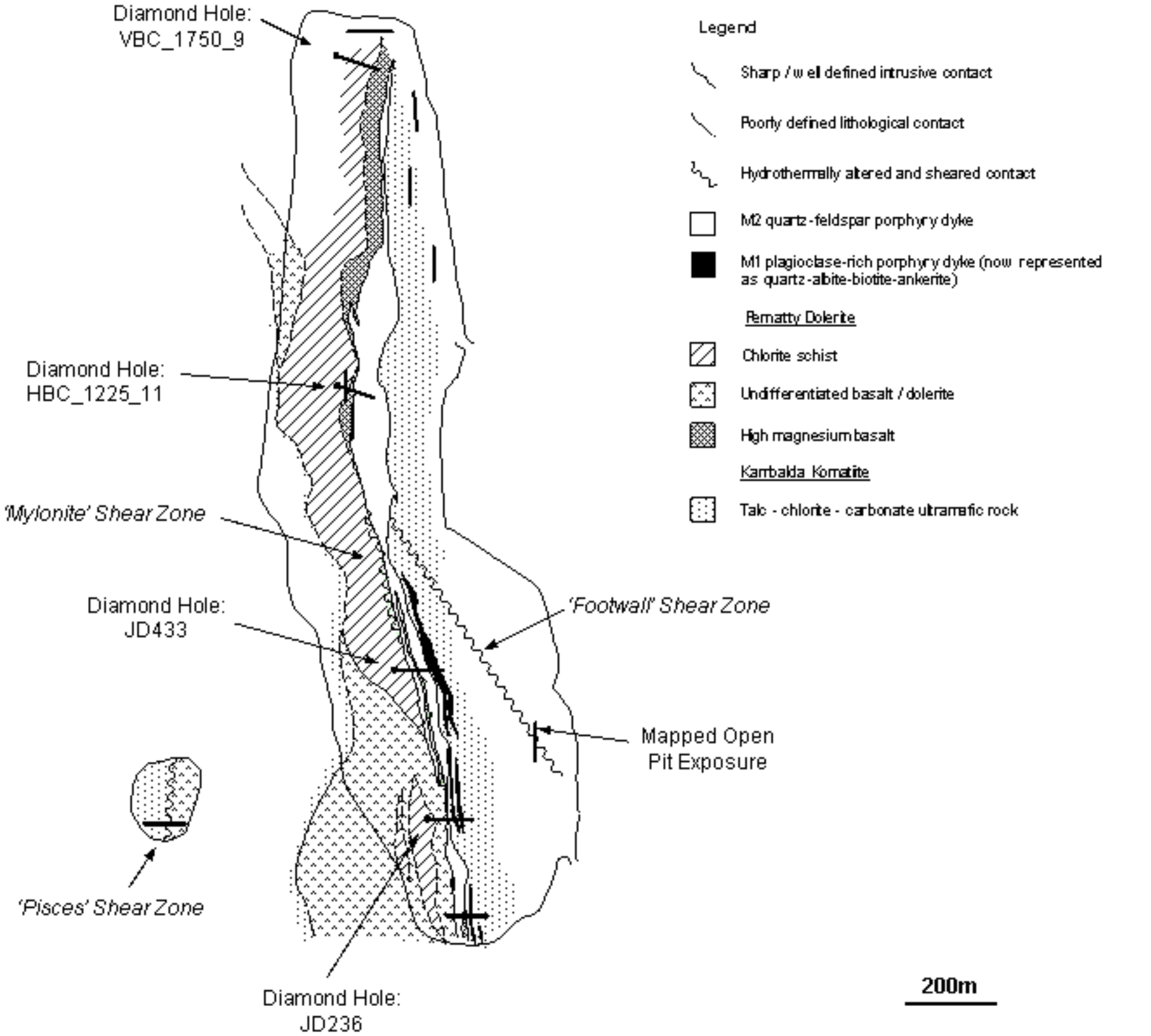

Figure 2B: Solid geology interpretation of the Hampton Boulder Jubilee deposit illustrating the distribution of major rock types. Interpretation is based on the mapping of open pit exposures and logging of diamond drill core by the authors, the positions of which are marked.

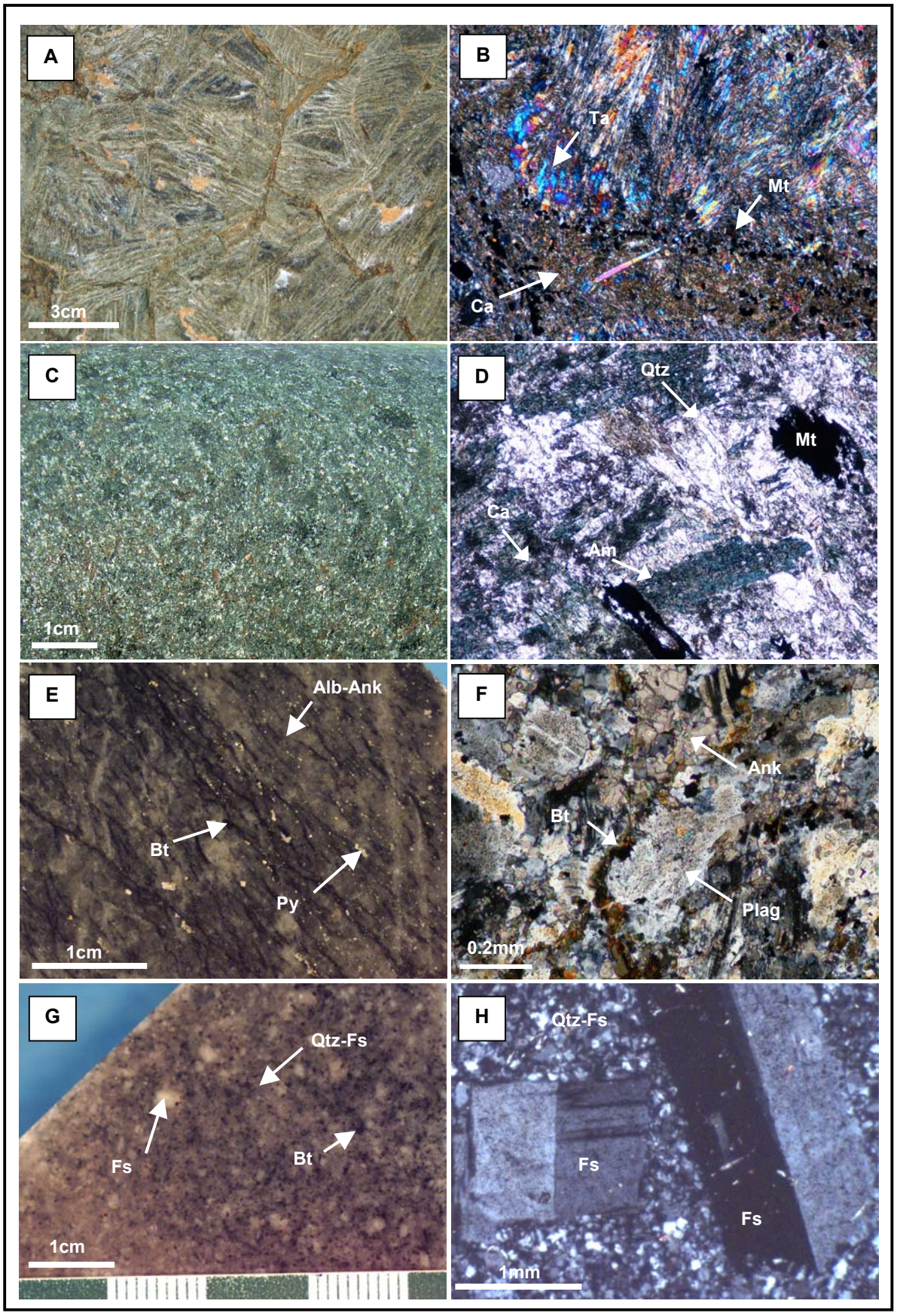
A
3cm
B
Ta
Mt
Ca
C
1cm
D
Qtz
Mt
Ca
Am
E
Alb-Ank
Bt
Py
1cm
F
Ank
Bt
Plag
0.2mm
G
Qtz-Fs
Fs
Bt
1cm
H
Qtz-Fs
Fs
Fs
1mm

Figure 3: Photographs and thin section photomicrographs illustrating the host rocks of the New Celebration gold deposits:

A. Random spinifex texture preserved in altered Kambalda Komatiite, sample from the ultramafic footwall, Hampton Boulder open pit, 340 – 350rl.
B. Thin section photomicrograph captured at x5 magnification (cross polarised light) of Kambalda Komatiite. Olivine has been replaced by hydrothermal magnetite, preserving relict spinifex textures and carbonate alteration is pervasive throughout the rock.
C. Hand specimen of least altered Pernatty Dolerite (Hanging wall dolerite, Hampton Boulder Jubilee) collected from diamond core JD236, 76m depth. Coarse-grained amphiboles are randomly aligned in a fine-grained quartz-plagioclase groundmass.
D. Thin section photomicrograph captured at x5 magnification (cross polarised light) of Pernatty Dolerite. Coarse-grained amphiboles contained in a fine-grained, quartz-plagioclase groundmass. Minor hydrothermal carbonate overprints the groundmass.
E. Hand specimen of M_1 porphyry now represented as quartz-biotite-ankerite schist showing anastomosing bands of biotite defining a lepidoblastic foliation (Sample from diamond core JD236, 144.0m depth)
F. Thin section photomicrograph of deformed and hydrothermally altered M_1 porphyry. Recrystallised plagioclase phenocrysts have been subsequently overprinted by biotite and ankerite.
G. Hand specimen of M_2 porphyry showing pale, cream coloured relict igneous phenocrysts of feldspar in a fine-grained quartz-feldspar-biotite groundmass. Sample from diamond core HBC_1225_11, 257.85m depth).
H. Thin section photomicrograph of twinning in relict igneous feldspar laths of the M_2 porphyry. Photomicrograph captured at x5 magnification under cross polarised light.

Abbreviations: Alb – Albite, Am – Amphibole, Ank – Ankerite, Bt – Biotite, Ca – Carbonate, Fs – Feldspar, Mt – Magnetite, Py – Pyrite, Qtz – Quartz, Ta - Talc

porphyry dykes and are thus attributed to a later magmatic event. The M_1 plagioclase-rich dykes intrude the ultramafic footwall and the sheared and hydrothermally altered mafic-ultramafic rock contact and form thin (50cm – 5m), 'ribbon-like' bodies boudinaged at depth and along strike. Intense hydrothermal alteration and deformation has obliterated primary igneous mineralogy and texture; these rocks are now represented as fine-grained quartz-biotite-albite-ankerite schists (Figure 3E and 3F). The mine sequence at Hampton Boulder Jubilee is dominated by a large, boudinaged M_2 quartz-feldspar porphyry dyke that intrudes the mafic hanging wall and the mafic-ultramafic rock contact. This dyke attains a maximum thickness of approximately 80m in the northern half of the Hampton Boulder Jubilee deposit and is persistent along strike having been traced southwards to the Golden Hope deposit. In hand specimen the M_2 porphyry is medium grey and locally contains aggregates of fine-grained biotite after amphibole (Figure 3G). Primary igneous textures are well preserved in M_2 porphyry dykes with coarse-grained (0.5mm – 2.0mm), lath-shaped phenocrysts of orthoclase randomly aligned in a fine-grained (<0.2mm) groundmass of quartz and feldspar (Figure 3H).

METHODOLOGY

Detailed structural (dip angle and dip direction convention) and hydrothermal alteration mapping of accessible exposures was completed in the Hampton Boulder Jubilee and Jubilee West open pits. The majority of mapping was completed at 1:250 scale with two key exposures, the north face and south face exposures in the Hampton Boulder Jubilee open pit mapped at 1:100 scale. Oriented thin sections for microstructural investigation were prepared from hand samples collected in the open pits.

The structural location of gold and identification of mineralisation styles was determined macroscopically by diamond core logging in conjunction with open pit mapping. The locations of open pit exposures mapped and diamond cores logged are represented in Figure 2. High grade ore zones were initially identified using company geochemical data whereas detailed re-sampling, petrography and fire assay of 8 - 20cm intervals of ore zones in the porphyry dykes by the authors further constrained the ore zones, host structures and associated hydrothermal alteration assemblages. Forty-nine polished thin sections representative of each gold mineralisation style and associated alteration zones were prepared from diamond core. The petrology of hydrothermal alteration and mineralization zones was determined by transmitted and reflected light microscopy of polished thin sections, qualitative microanalysis using a Leo 1550 Variable Pressure Scanning Electron Microscope and quantitative Energy Dispersive System (EDS) microanalysis using a Jeol 6400 Scanning Electron Microscope at the Centre for Microscopy and Microanalysis, University of Western Australia.

STRUCTURAL EVOLUTION

The New Celebration deposits are located within the Boulder segment of the Boulder-Lefroy fault zone, a major north-northwest trending, transcrustal fault zone (Weinburg et al., 2003; Swager et al., 1992). Structures mapped at the New Celebration deposits were attempted to be correlated with the regional D_1 to D_4 deformation events. However, because the current structural analysis of the New Celebration deposits is restricted to the near-mine area, the correlation with regional deformation events cannot always be rigorously demonstrated. Therefore, the subscript $_{NC}$ is used to equivocally distinguish structural elements observed at

New Celebration from regional structural features (e.g. Swager et al., 1995; Weinburg et al., 2003). Four deformation events are observed at New Celebration, the earliest being the D_{2NC} event. Structures correlating to the regional D_1 deformation event are not recognised on a mine scale at New Celebration.

Deformation Event D_{2NC} – Formation of upright folds

STRUCTURES

The earliest deformation event recognised at New Celebration is D_{2NC} represented by the tilting of conformable stratigraphic contacts to near-vertical orientations. Examples include contacts between sub-units of the differentiated dolerite unit exposed in the south face wall of the Hampton Boulder Jubilee open pit (Figure 4).

Deformation Event D_{3NC} – Formation of NNW trending shear zones

STRUCTURES

A north northwest-trending penetrative foliation, elongation lineations, S-C intersection lineations and slickenline lineations represent the D_{3NC} deformation event. The penetrative S_{3NC} foliation has sub-millimetre spacing and is observed in mafic and ultramafic rocks, defined by chlorite and talc, respectively. Within the northern half of the Hampton Boulder Jubilee open pit, the S_{3NC} foliation has an average orientation of 78^o towards 248^o, although a large variation in the orientation of strike and dip is observed (Figure 5). Within the southern half of the Hampton Boulder Jubilee deposit deformation is concentrated into 10m – 50m wide, intensely foliated, high-strain zones. In cases of extreme high strain, rock textures are mylonitic with small (<0.5mm), boudinaged quartz-ankerite lenses surrounded by anastomosing biotite-sericite laminae.

An S-C fabric is well developed in both the mafic rocks and M_1 porphyry dykes, however, it is not observed in ultramafic rocks due to the obliteration of deformation fabrics by late overprinting actinolite-tremolite and carbonate. The S-foliation trends north-northwest and has an average orientation of 82^o towards 260^o, whereas the C-foliation has an average orientation of 87^o towards 229^o (Figure 5). Microscopic features, including the relationship between S- and C-foliation planes and the orientation of sigmoidal quartz veins, indicate a top-to-the-right sense of movement, which corresponds to movement down-plunge of the south-southwest plunging mineral elongation lineation.

Mineral elongation lineations (L_{3mNC}), S-C intersection lineations (L_{3iNC}) and slickenline lineations (L_{3sNC}) on fault surfaces are identified in all exposures mapped in the Hampton Boulder Jubilee open pit. Mineral elongation lineations (L_{3mNC}) developed in the mafic and ultramafic hydrothermally altered schistose rocks plunge at moderate to steep angles towards the south-southwest to south-southeast (Figure 5). Intersection lineations (L_{3iNC}) between the S- and C-foliation planes are developed in ultramafic and mafic rocks and plunge at moderate to steep angles towards the northwest (Figure 5). Slickenline lineations (L_{3sNC}) plunge at moderate to steep angles towards the south-southeast to south-southwest and are developed on brittle fault planes in intermediate intrusive rocks and at the margins of boudinaged, S_{3NC} foliation-parallel quartz-carbonate veins.

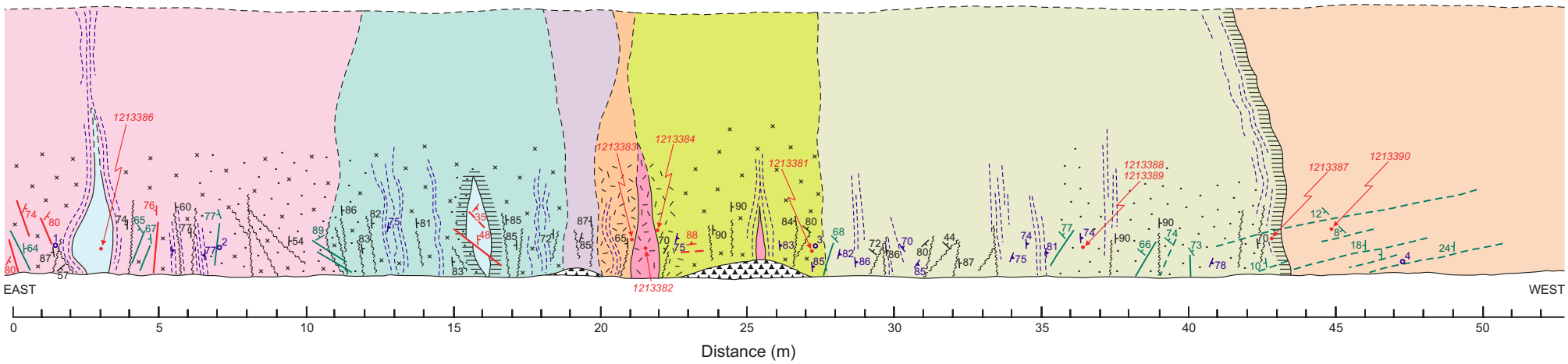

LITHOLOGY

- Talc-chlorite-carbonate ultramafic rock
- Talc-chlorite-carbonate ultramafic schist
- Dolerite, containing disseminated magnetite
- Chlorite ± biotite schist
- Dolerite with discrete shear zones (chlorite schist)
- Biotite schist
- Unsheared quartz-feldspar porphyry
- Sheared porphyry, biotite altered
- Mafic intrusive
- Rubble

ALTERATION

- Disseminated (± euhedral) fine grained magnetite
- Disseminated, euhedral pyrite
- Decussate, coarse-grained amphibolite
- Intense chlorite alteration

SYMBOLS

- 85 Dip and dip direction of shear plane
- Dip direction (dip not measured) of shear plane
- 83 Dip and dip direction of foliation
- 48 Dip and dip direction of fault
- 89 Dip and dip direction of vein
- 88 Dip and dip direction of joint surface
- 3 Indicates position of blow-up diagrams
- 1213382 Sample number

CONTACTS, STRUCTURES

- Sharp intrusive contact
- Diffuse/poorly defined contact
- Shear plane/shear zone
- Trace of foliation
- Fault
- Joint surface
- Quartz-carbonate vein
- Massive quartz vein

SHf001-04

Figure 4: Detailed geological map of the northern open-pit wall of the Hampton Boulder-Jubilee open pit. This map represents a cross-section through the deposit and the Boulder-segment of the Boulder-Lefory fault zone which controls the location of most of the open pits at New Celebration (see Figure 2A)

BELOW: Poles to S_{3MC} foliation planes measured in the mafic hangingwall. Foliation has an average trend of 82°→254° (n=41)

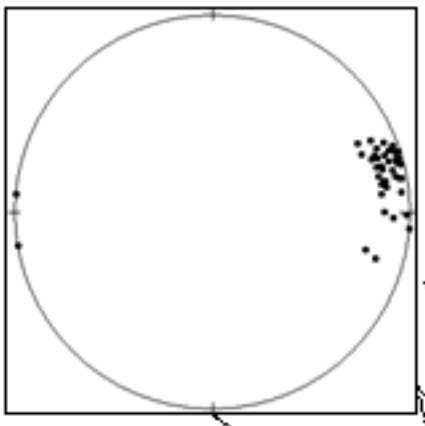

RIGHT: Mineral elongation lineations, L_{3mMC} from the Hampton Boulder Jubilee open pit (n=15).

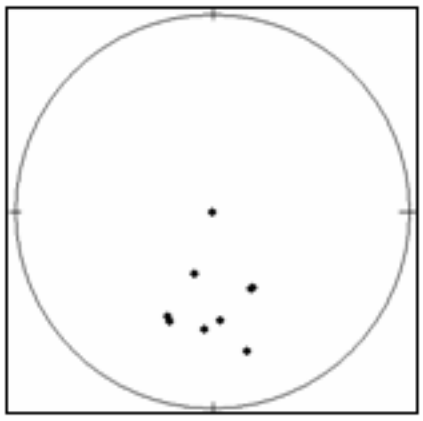

BELOW: Poles to S_{3MC} foliation planes measured in the ultramafic footwall. Foliation has an average trend of 70°→250° (n=102).

BELOW RIGHT: Intersection lineations, L_{3MC} from the Hampton Boulder Jubilee open pit (n=48).

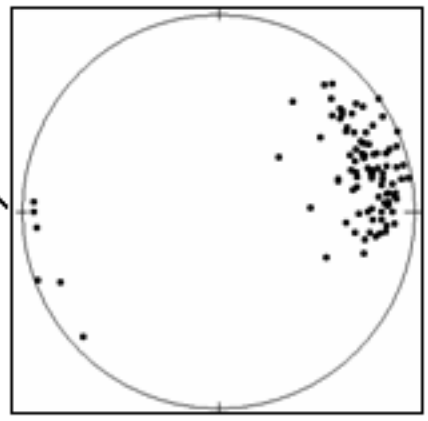

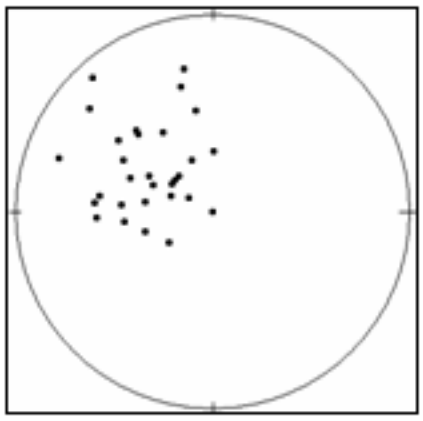

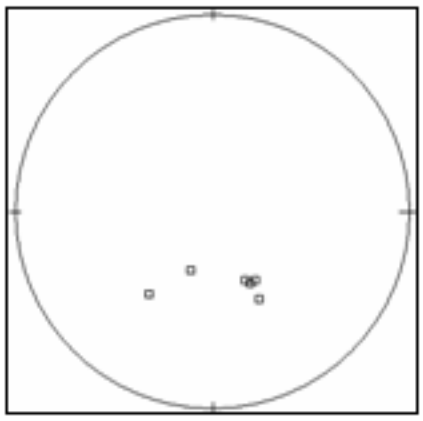

ABOVE: Slickenline lineations, L_{3mMC} from the Hampton Boulder Jubilee open pit (n=6).

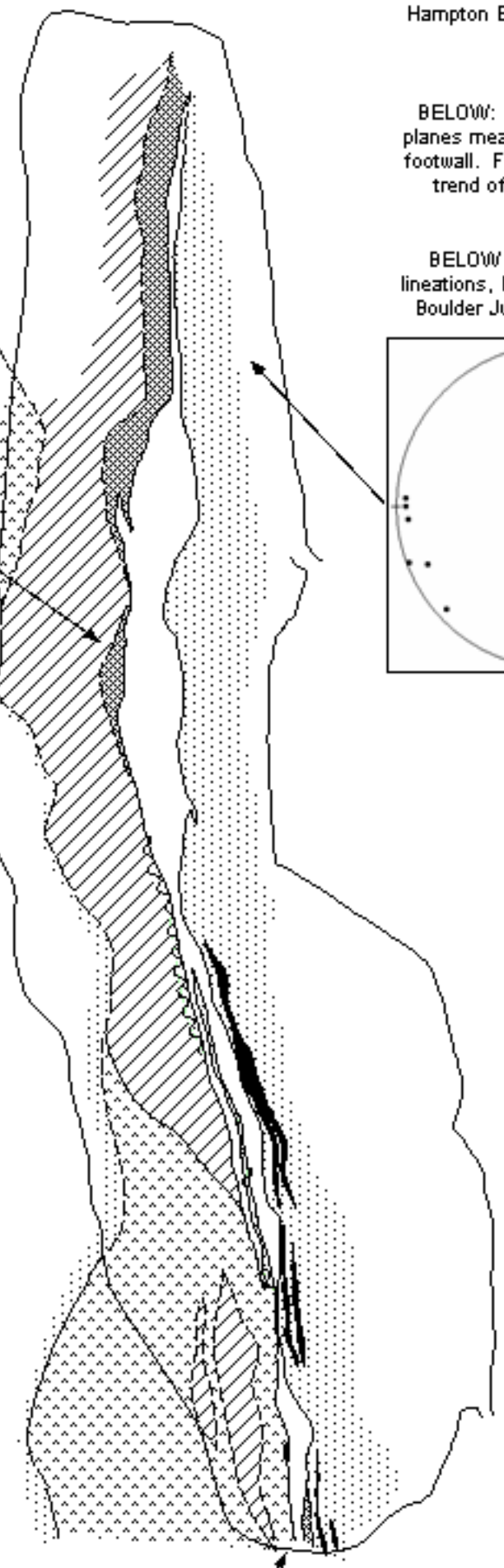

200m

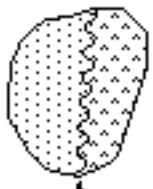

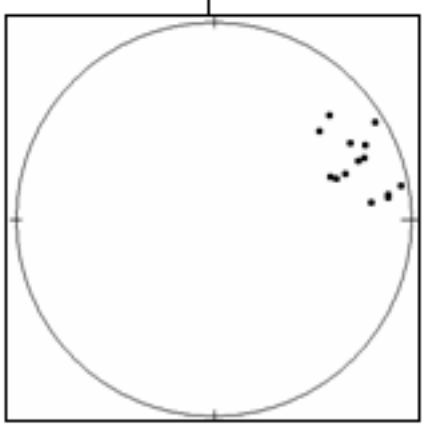

ABOVE: Poles to S_{3MC} foliation planes measured in the Jubilee West open pit. Foliation has an average trend of 73°→248° (n=14)

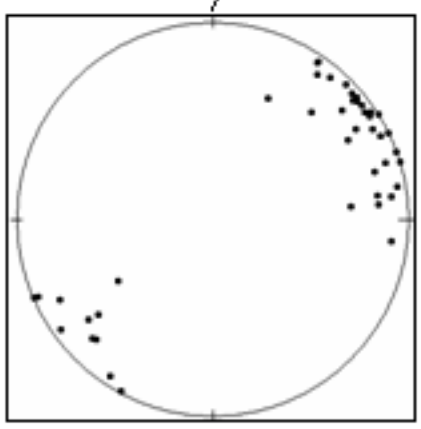

ABOVE: Poles to S_{3MC} foliation planes measured in the HBJ south-face open pit exposure. S-Foliation planes have an average trend of 83°→261°, C-Foliation, 87°→229° (n=43).

Legend

- Sharp / well defined intrusive contact
- Poorly defined lithological contact
- Hydrothermally altered and sheared contact
- M2 quartz-feldspar porphyry dyke
- M1 plagioclase-rich porphyry dyke (now represented as quartz-albite-biotite-ankerite)

Pernatty Dolerite

- Chlorite schist
- Undifferentiated basalt / dolerite
- High magnesium basalt

Karrbalda Komatiite

- Talc - chlorite - carbonate ultramafic rock

Figure 5: Summary of structures relating to the D_{3NC} deformation event taken from different domains within the Hampton Boulder Jubilee and Jubilee West open pits. Structural data is presented on equal area (southern hemisphere) stereonet projections. The S_{3NC} foliation planes trend NNW and dip steeply towards the WNW. The L_{3mNC} mineral elongation lineations plunge at moderate to steep angles towards the SSW to SSE, L_{3iNC} S-C intersection lineations plunge at moderate angles towards the northwest and L_{3sNC} slickenline lineations plunge at moderate angles towards the SSW to SSE.

NATURE OF DEFORMATION:

A predominance of moderate- to steep south-southwest plunging mineral elongation lineations, combined with the north-northwest trending, west-dipping S_{3NC} foliation suggests that movement on the fault zone was dominantly oblique-slip. Using the orientation of S-C fabrics and the sigmoidal shape of deformed quartz grains the movement was constrained to be down-plunge of the lineation indicating that the movement on the shear zone during D_{3NC} deformation was sinistral oblique-slip, west-block-down movement towards the south-southwest.

Deformation Event D_{4NC} – Formation of NNE trending shear zones

STRUCTURES

Structures relating to the D_{4NC} deformation event are preferentially developed in the ultramafic footwall and mafic hangingwall and correlate to the regional D_4 compressive deformation described by Swager (1995) (Figure 6). The S_{4NC} foliation has two main orientations, 81^o towards 312^o and 58^o towards 292^o (Figure 6) which represent the S- and C-foliation planes of a penetrative S-C fabric developed during D_{4NC} deformation.

North-northeast trending structures are locally observed in the south face exposure of the Hampton Boulder Jubilee open pit cross cutting the S_{3NC} foliation (Figure 4). These D_{4NC} structures have an average orientation of 62^o towards 243^o (Figure 6) and are filled with quartz-carbonate-epidote-chlorite veins up to 3cm in width. Slickenline lineations, L_{4sNC}, developed at the vein margins indicate that these structures represent vein-filled faults. These lineations have an average plunge of 6^o towards 213^o and are indicative of strike slip deformation. No kinematic indicators were observed, therefore, the direction of fault movement cannot be constrained.

Two sets of steeply west to north-northwest dipping quartz-carbonate$\pm$chlorite veins, V_{4aNC} and V_{4bNC}, cross cut D_{3NC} deformation fabrics and have orientations of approximately 67^o towards 346^o and 64^o towards 314^o, respectively (Figure 6).

NATURE OF DEFORMATION:

Horizontal L_{4sNC} slickenline lineations developed at the margins of north-northeast trending V_{4NC} quartz-carbonate-epidote-chlorite veins indicate strike-slip movement although, due to lack of kinematic indicators, the exact motion on D_{4NC} faults cannot be determined.

Deformation Event D_{4+nNC} – Formation of brittle, west-dipping structures

STRUCTURES

Structures formed during the D_{4+nNC} deformation event are poorly represented in the open pits. A curviplanar fault observed in the Hampton Boulder Jubilee south face exposure has an orientation of 48^o towards 235^o (Figure 4) and cross-cuts a boudinaged, S_{3NC} foliation-parallel biotite lamprophyre dyke (Figure 4). A fault of similar morphology is observed in the north face exposure of the Hampton Boulder Jubilee open pit dipping moderately towards the west and offsetting a boudinaged V_{3NC} quartz-carbonate vein. Due to the lack of exposure and access, the apparent offset on, and true orientation of the fault could not be determined.

Cross-cutting relationships with D_{3NC} structures constrain the timing of these faults as post-D_{3NC}. In addition, the orientation of west-dipping curviplanar faults is significantly different to that of D_{3NC} and D_{4NC}

structures (S_{3NC} foliation, 83° towards 239°; S_{4NC} foliation, 58° towards 292° and 81° towards 312°). Based on these observations, the timing of these faults is tentatively constrained as post-D_{4NC} deformation, and therefore, west-dipping faults represent D_{4+nNC} deformation.

Morphology and Timing of Post-D_1 Intrusive Rocks

The M_1 porphyry dykes have intruded the ultramafic footwall and the sheared mafic-ultramafic rock contact and form thin (50cm – 5m) 'ribbon-like' bodies' boudinaged both down dip and along strike. Primary igneous textures have been replaced by the penetrative S_{3NC} foliation defined by biotite; an S-C fabric is also locally observed. The development of D_{3NC} deformation fabrics suggests the intrusion of these porphyries occurred pre- or syn-D_{3NC} deformation. However, in the absence of geochronological data or cross cutting relationships between M_1 porphyry dykes and D_{2NC} structures, the timing of these porphyries may not be constrained further. All M_1 porphyry dykes show evidence of recrystallisation of the quartz-plagioclase groundmass (Figure 7A).

The M_2 porphyry dykes are persistent along strike and intrude the sheared and hydrothermally altered mafic-ultramafic rock contact, and, like the M_1 porphyry dykes, are boundinged down dip and along strike. The penetrative north-northwest trending S_{3NC} foliation is observed wrapping around M_2 quartz-feldspar porphyry dykes which suggests that intrusion, and subsequent deformation of M_2 porphyry dykes, occurred synchronous with the D_{3NC} sinistral, oblique-slip deformation event. In contrast to M_1 porphyry dykes, igneous minerals and textures are well preserved in M_2 porphyry dykes and there is no evidence for recrystallisation (Figure 7B). The M_2 porphyry dykes have, however, undergone brittle deformation resulting in the development of a brittle fracture network at the margins of the porphyry (Figure 7C) including brittle deformation of phenocrysts (Figure 7D). The timing of these fractures is somewhat equivocal. These fractures could represent the expression of D_{3NC} deformation in a more competent rock type, where compared to the less competent mafic and ultramafic host rocks, or a subsequent brittle deformation event post-dating D_{3NC} deformation. There is a distinct lack of D_{4NC} structures cross cutting the boudinaged M_2 quartz-feldspar porphyry, which, however, does not preclude the intrusion of the porphyry dykes prior to this event as structures developed in the less competent mafic and ultramafic schists may not be manifested in the more competent porphyry.

GOLD MINERALISATION STYLES AND ASSOCIATED HYDROTHERMAL ALTERATION

Four structurally controlled gold mineralisation styles have been identified at New Celebration, the timing of which is directly related to the outlined deformation events. Gold is predominantly hosted in two generations of porphyry dykes, M_1 plagioclase-rich and M_2 quartz-feldspar porphyry dykes, and in high-magnesium basalt of the mafic hangingwall. The defining characteristics of the gold mineralisation styles are summarised in Table 2.

BELOW: Poles to V_{4sNC} and V_{4bNC} quartz-carbonate veins measured in the mafic hangingwall of the Hampton Boulder Jubilee open pit.

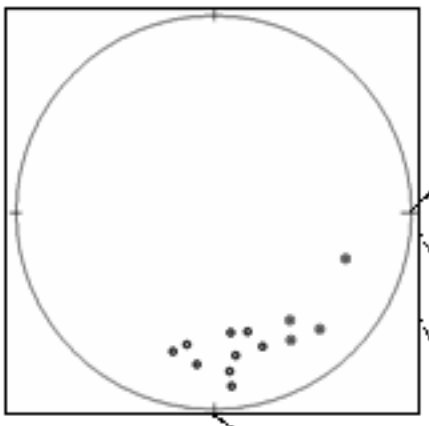

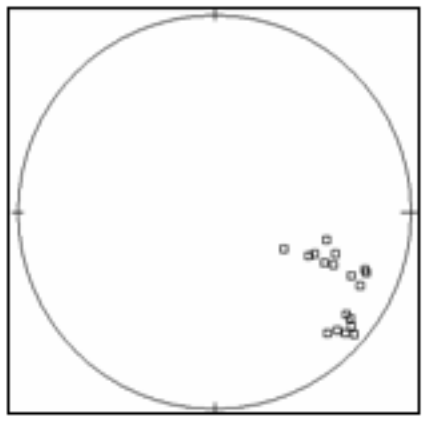

ABOVE: Poles to S_{4NC} foliation planes in the Hampton Boulder Jubilee open pit (n=18).

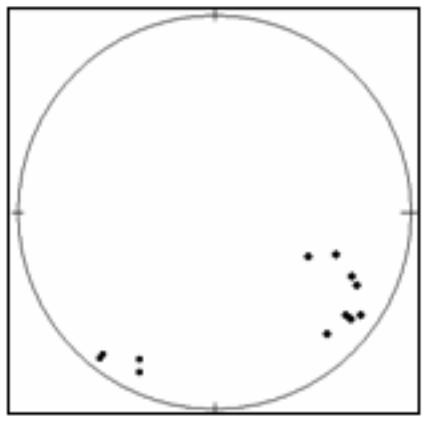

ABOVE: L_{4sNC} slickenline lineations (circles) and poles to D_{4NC} fault planes (diamonds) on which they are developed (n=12) .

200m

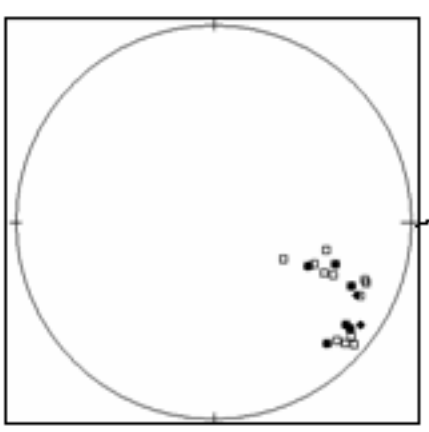

LEFT: Poles to S_{4NC} foliation planes (open squares) and D_{4NC} quartz-carbonate-epidote-chlorite, vein-filled faults (filled diamonds) in the Hampton Boulder Jubilee open pit (n=26).

Legend

- Sharp / well defined intrusive contact
- Poorly defined lithological contact
- Hydrothermally altered and sheared contact
- M2 quartz-feldspar porphyry dyke
- M1 plagioclase-rich porphyry dyke (now represented as quartz-albite-biotite-ankerite)

Fortescue Group

- Chlorite schist
- Undifferentiated basalt / dolerite
- High magnesium basalt

Kambalda Komatiite

- Talc - chlorite - carbonate ultramafic rock

Figure 6: Summary of structures relating to the D_{4NC} deformation event. Structural data is presented on equal area (southern hemisphere) stereonet projections. The S_{4NC} foliation planes trend NNE and dip steeply towards the WNW. Subhorizontal L_{4sNC} slickenline lineations plunge towards the SE. Two sets of steeply west to north-northwest dipping quartz-carbonate±chlorite veins, V_{4aNC} and V_{4bNC}, cross cut D_{3NC} deformation fabrics and dip steeply (>60^{o}) towards 346^{o} and 314^{o}, respectively

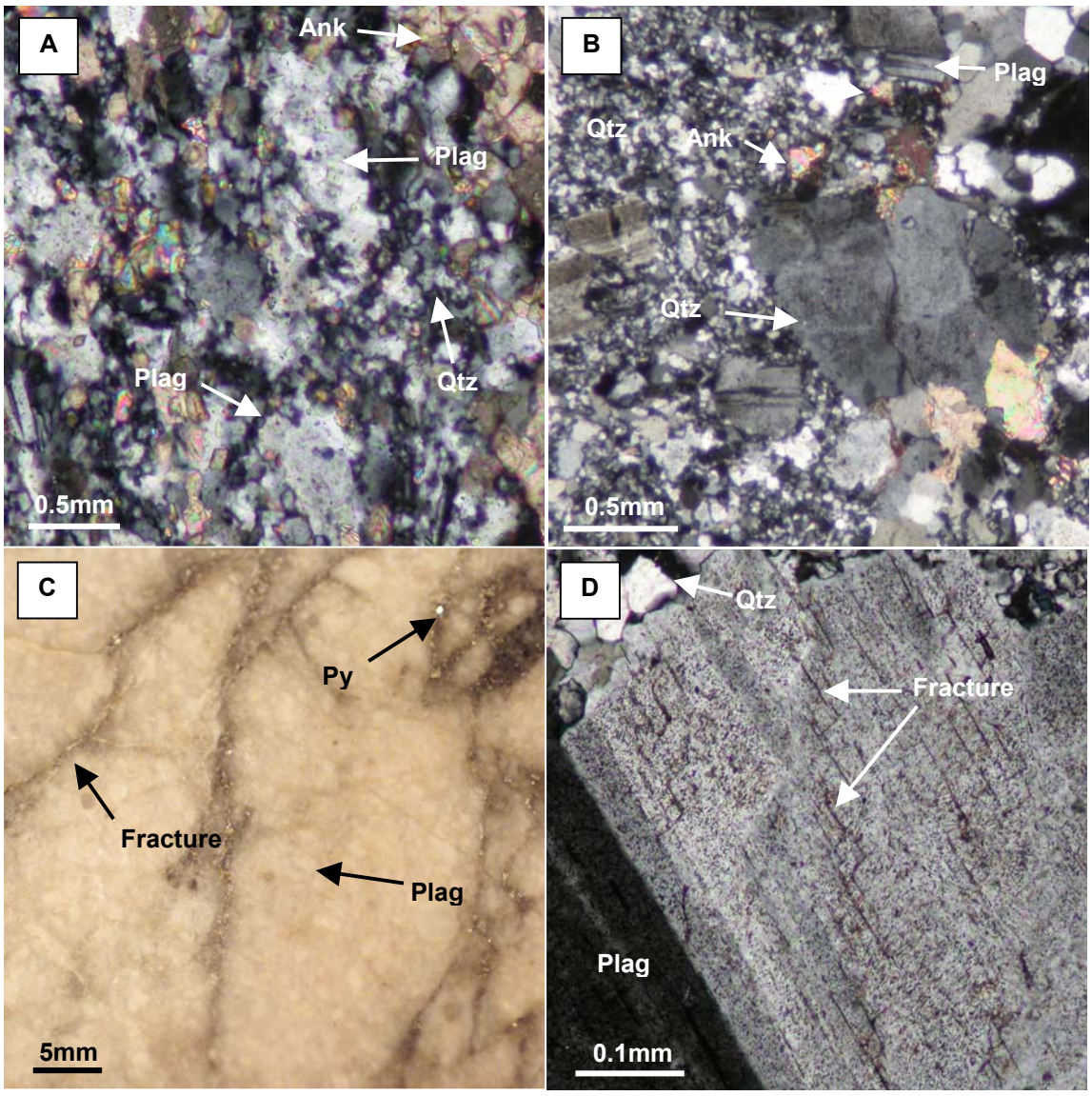

Abbreviations: Ank – Ankerite; Plag – Plagioclase; Py – Pyrite; Qtz – Quartz

Figure 7: Photoplate of internal textures and microstructures of the M_1 plagioclase-rich and M_2 quartz-feldspar porphyry dykes:

A. Photomicrograph of internal texture of M_1 plagioclase-rich porphyry. Both the plagioclase phenocrysts and the fine-grained quartz-plagioclase groundmass have undergone grainsize reduction and recrystallisation (x10 magnification).
B. Photomicrograph showing internal textures of M_2 quartz-feldspar porphyry. The quartz and feldspar phenocryst grain boundaries are pristine and show little evidence of recrystallisation (x5 magnification).
C. Fractures developed in M_2 quartz-feldspar porphyry dykes.
D. Photomicrograph of a plagioclase phenocryst in M_2 quartz-feldspar porphyry with brittle en echelon fractures (x5 magnification).

'Early' Gold Mineralisation and Related Hydrothermal Alteration

MYLONITE-STYLE:

Mylonite-Style gold mineralisation is hosted within the high-strain quartz-ankerite-biotite-sericite mylonite zone located in the mafic hangingwall in the northern part of the Hampton Boulder Jubilee deposit. The equilibrium mineral assemblage biotite-sericite-ankerite±pyrite±magnetite characterises the distal alteration zone of Mylonite-style gold mineralisation with hydrothermal quartz, pyrite and magnetite present as minor constituents (Table 2; Figures 9 and 10A). Fine-grained (<0.01mm), elongate biotite and sericite define the well developed S_{3NC} foliation in the distal alteration zone and are inter-layered with lenses of fine-grained, recrystallised quartz and anhedral, fine- to medium-grained (<0.02 – 0.2mm) metasomatic ankerite (Figure 10A). Fine-grained magnetite and pyrite is commonly fractured and is disseminated throughout the groundmass (Figure 10A).

The proximal alteration assemblage is defined by the equilibrium assemblage ankerite-biotite-pyrite±sericite and the complete replacement of magnetite by pyrite (Table 2; Figure 9). Gold, galena and the gold±silver tellurides calerverite ($AuTe_2$) and petzite (Ag_3AuTe_2) are present as small (1-2µm) rounded inclusions in anhedral pyrite grains (Figure 10B). Gold also occurs in equilibrium with the lead telluride altaite (PbTe) as fine-grained (1-2µm) anhedral grains disseminated within the silicate gangue adjacent to the margins of anhedral pyrite grains (Figure 10C).

PORPHYRY-STYLE

Porphyry-Style gold mineralisation is restricted to M_1 plagioclase-rich porphyry dykes that have intruded the footwall and sheared contact in the southern half of the Hampton Boulder Jubilee deposit. All M_1 porphyries are pervasively hydrothermally altered and mineralised, and lack distinct alteration zones. The equilibrium mineral assemblage albite-biotite-pyrite-ankerite±sericite characterises the hydrothermally altered M_1 porphyry (Table 2; Figure 10D), with chalcopyrite, galena, hematite, magnetite, monazite, tellurides and gold present as minor constituents. Fine-grained (<0.01mm), anhedral, metasomatic biotite defines the S_{3NC} foliation and, locally, the D_{3NC} S-C fabric. Albite is medium-grained (0.5 - 2mm) and anhedral in texture and is overprinted by polygranular aggregates of ankerite (Figure 10D). Disseminated pyrite ranges in grainsize from 0.1 – 2mm and is in textural equilibrium with biotite.

Magnetite and haematite occur as sub-rounded inclusions within pyrite, whereas specular haematite overprints all subsequent hydrothermal alteration minerals (Figure 10E). Gold is present in a variety of forms: (1) small (1 to 2µm), rounded inclusions within anhedral pyrite; (2) very fine-grained, anhedral disseminated grains along albite grain boundaries and in close proximity to pyrite; (3) anhedral, sub-rounded grains deposited along fractures in anhedral pyrite; and 4) subhedral crystals located in cavities in euhedral pyrite and in equilibrium with the tellurides hessite ($AgTe_2$), altaite (PbTe), melonite (Ni_2Te) and tetradymite (Bi_2Te_2) (Figure 10F).

STRUCTURAL LOCATION

Gold associated with both Mylonite-Style and Porphyry-Style gold mineralisation is associated with tellurides species and is hosted within pyrite. Structurally, host pyrite is aligned parallel with the north-northwest trending S_{3NC} foliation planes (Table 2), whereas pressure shadows of ankerite and hydrothermal quartz are

developed at the margins of host pyrite and indicate the precipitation of pyrite and gold prior to, or synchronous with D_{3NC} deformation.

'Late' Gold Mineralisation and Related Hydrothermal Alteration

CONTACT-STYLE

Contact-Style gold mineralisation is hosted within high-magnesium basalt adjacent to the intrusive contact with M_2 quartz-feldspar porphyry dykes. Contact-Style gold mineralisation comprises three main zones of alteration: (1) ankerite-biotite-chlorite alteration occurs distal to the ore bodies. Fine-grained (<0.05mm) chlorite and biotite define the well-developed penetrative S_{3NC} foliation, whereas ankerite forms polygranular aggregates that locally overprint biotite and chlorite (Figure 12A). Magnetite occurs in two forms: (a) disseminated aggregates of fine-grained, zoned, euhedral grains, and (b) disseminated, fine-grained, anhedral crystals, variably replaced by pyrite; (2) ankerite-biotite-sericite alteration zone. Magnetite is not stable within this zone, having been completely replaced by anhedral to euhedral pyrite disseminated throughout the groundmass; (3) ankerite-sericite alteration reflects the proximal alteration and is the host to gold (Figure 12B). The proximal alteration zone occurs adjacent to the contact with M_2 porphyry dykes and reflects the progressive replacement of biotite by sericite; this zone is also characterised by high modal percentages of pyrite (up to 80%) (Figure 11).

Gold is disseminated and occurs as: (a) small, rounded inclusions contained within pyrite, and (b) anhedral grains attached to, or adjacent to the margins of disseminated pyrite grains (Figure 12C). Haematite and rutile occur only as minor accessory phases.

FRACTURE-STYLE

Fracture-Style gold mineralisation is restricted to fractures developed only within M_2 quartz-feldspar porphyry. Two alteration zones are recognised: (1) a distal alteration zone represented by widespread pervasive ankerite-sericite alteration. Ankerite and sericite form only minor constituents of the rock (typically <5%), in which relict igneous minerals and textures are well preserved (Figure 12D), and (2) a proximal alteration zone characterised by the equilibrium assemblage pyrite-sericite-ankerite and restricted to the fracture filling material (Figure 13). Pyrite forms subhedral to euhedral, fine- to coarse-grained (<0.1 to 3mm) crystals (Figure 12E) which occur in textural equilibrium with fine-grained sericite and ankerite. Gold, galena and barite are present as small (1 to 5µm), sub-rounded inclusions in pyrite (Figure 12F) and as sub-rounded grains attached to the margins of pyrite crystals

STRUCTURAL LOCATION

Gold associated with 'Contact' gold mineralisation style is located: (1) attached to pyrite grains developed at the contact between high-magnesium basalt and M_2 quartz-feldspar porphyry; and (2) associated with, and hosted within disseminated pyrite aligned parallel to S_{3NC} foliation planes wrapping around the margins of M_2 quartz-feldspar porphyry.

Gold associated with 'Fracture' style gold mineralisation is hosted as inclusions within pyrite and as anhedral grains attached to the margins of pyrite within sericite-ankerite filled fractures. These fractures are

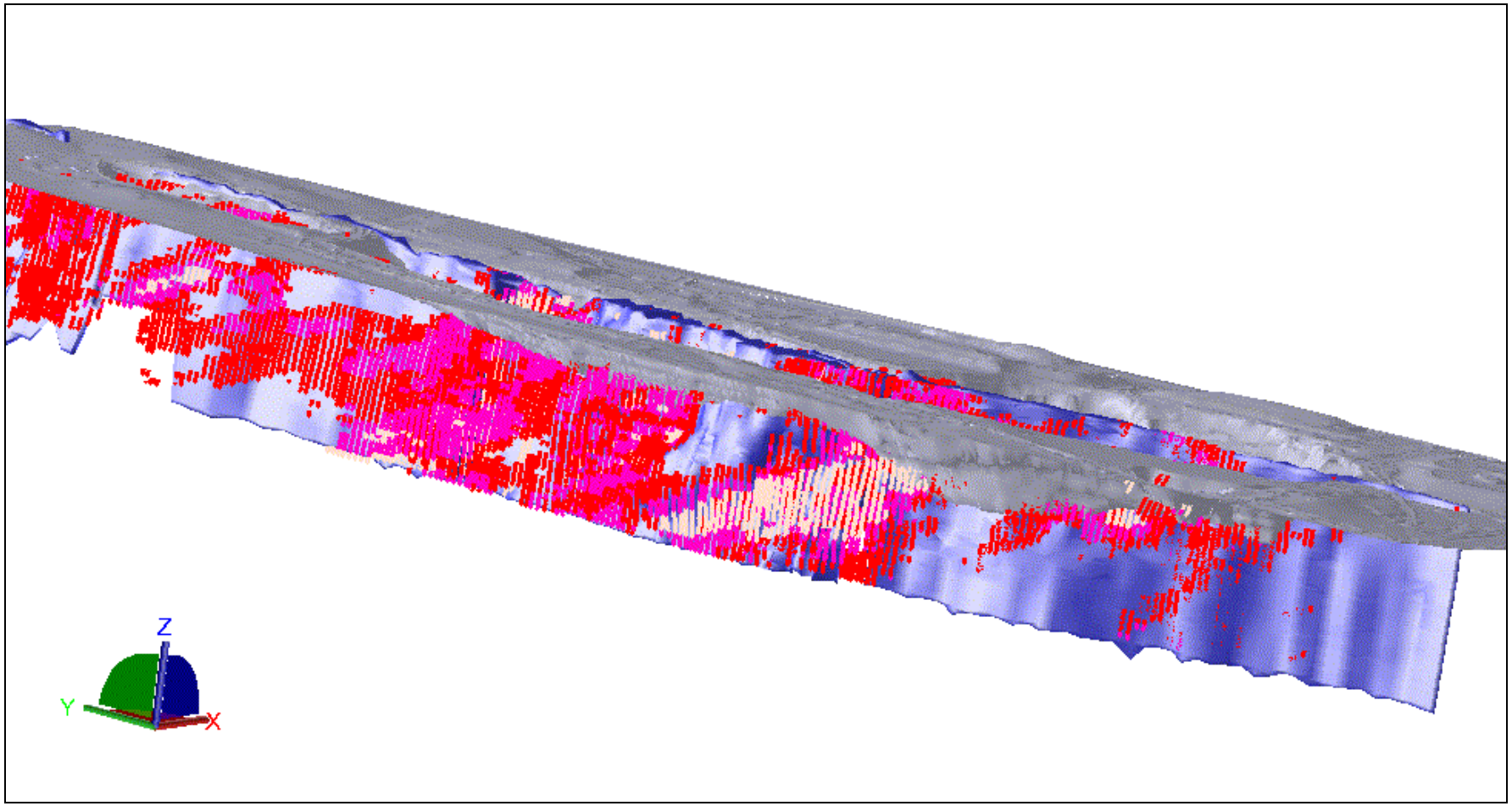
Z
Y
X

Figure 8: Block model of the Hampton Boulder Jubilee deposit showing ore zones (beige: +5g/t, pink: 2 – 5g/t, red: 1 – 2g/t) superposed on the M_1 porphyry dyke (blue); looking northeast. Ore zones are developed sub-parallel to the sheared and metasomatised mafic-ultramafic rock contact, which has been intruded by M_1 porphyry dykes. High-grade ore shoots, e.g. Southern Ore Zone, plunge moderately to steeply towards the northwest.

Mylonite-Style Gold Mineralisation

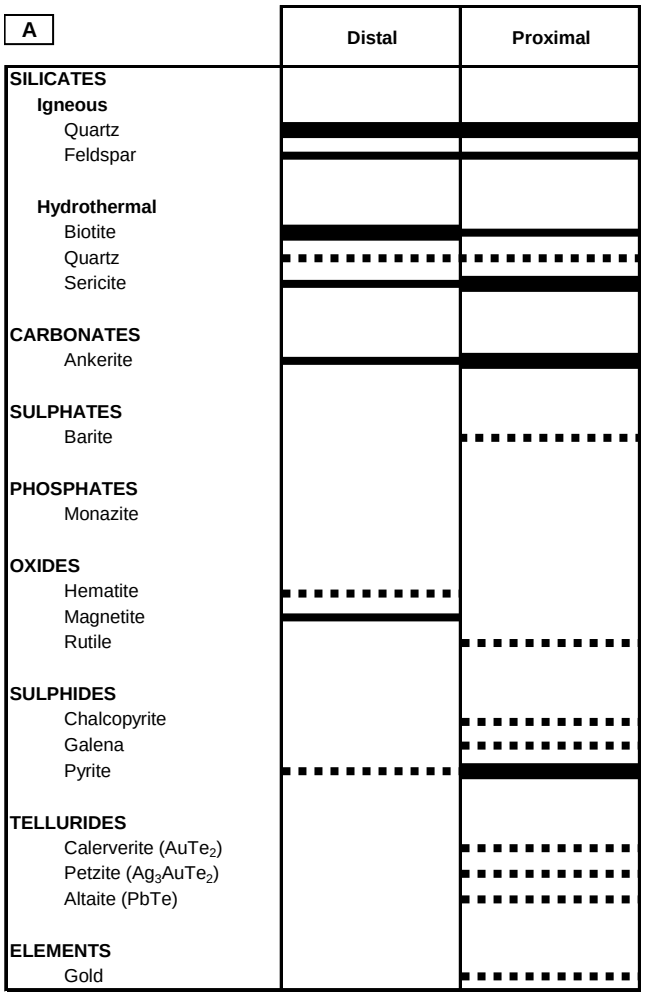

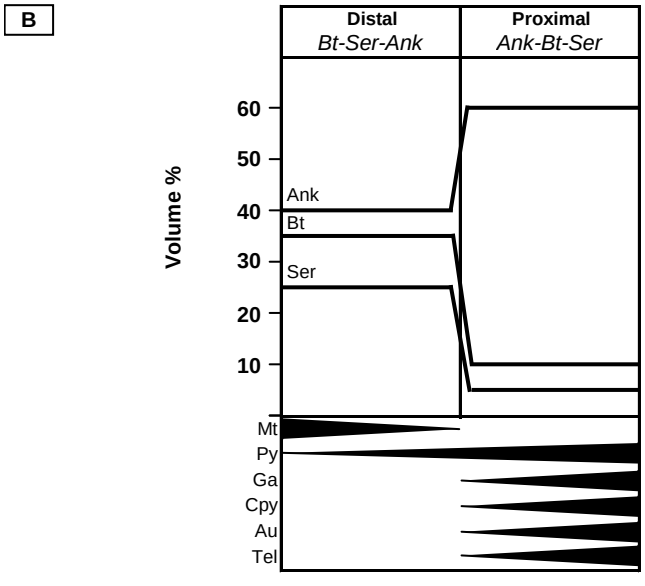

Figure 9A: Hydrothermal alteration zonation diagram illustrating changes in mineralogy across alteration zones of the ‘Mylonite-Style mineralisation. The distal alteration zone is characterised by the equilibrium assemblage biotite-sericite-ankerite with pyrite-magnetite present in trace proportions. The proximal alteration zone is characterised by: 1) increases in sericite and ankerite, 2) decreases in biotite, 3) absence of magnetite, and 4) the presence of gold and gold-silver bearing tellurides.

Figure 9B: Modal mineralogy of major and accessory minerals characteristic of the distal and proximal alteration zones of the ‘Mylonite’ gold mineralisation style. Major minerals are displayed as volume percent.

developed at the margins of boudinaged M_2 quartz-feldspar porphyry dykes during brittle deformation of the M_2 quartz-feldspar porphyry dykes.

STRUCTURAL AND HYDROTHERMAL ALTERATION MODEL

The integrated structural and hydrothermal alteration model for gold mineralisation at the New Celebration gold deposits presented here is based on the critical timing relationships between structure sets and lithological units, characteristic hydrothermal alteration minerals and their cross-cutting and replacement relationships observed in rocks from the Hampton Boulder Jubilee and Jubilee West open pits and diamond drill core. The model is separated into four structural stages/deformation events:

Stage 1: D_{2NC} deformation and intrusion of M_1 porphyry dykes and formation of Mylonite- and Porphyry-style gold lodes

The earliest deformation event, D_{2NC}, is represented by the tilting of conformable sub-units within the differentiated mafic hangingwall to near-vertical orientations.

Two post-D_1 magmatic stages have been invoked to explain the differences in the porphyry dykes observed in the open pits. Stage I magmatism is represented by thin, 50cm - 2m wide, M_1 plagioclase-rich porphyry dykes that have intruded the sheared and hydrothermally altered ultramafic-mafic rock contact and the ultramafic footwall adjacent to the contact zone. All M_1 porphyry dykes have undergone penetrative hydrothermal alteration and been subjected to intense non-coaxial deformation, as is evidenced by the well-developed S-C fabric (cf. Lister and Snoke, 1984) observed in all M_1 porphyry dykes. Recrystallised plagioclase grains in M_1 porphyry dykes (Figure 8A) are possibly indicative of deformation occurring at temperatures >500^{o}C (Voll, 1960; Vogler and Voll, 1981). The M_1 porphyry dykes are cross-cut by D_{3NC} structures; however there is no evidence to suggest that the intrusion of these porphyry dykes could not have occurred during D_{2NC} and prior to the onset of D_{3NC} deformation.

'Early' gold mineralisation (Mylonite-style and Porphyry-style) is associated with a ductile, high-strain deformation regime and may have occurred contemporaneously with the intrusion and subsequent deformation of the M_1 porphyry dykes (i.e. syn-D_{2NC}). However, structurally the two gold mineralisation styles are hosted within north-northwest trending S_{3NC} foliation planes and an early-D_{3NC} timing of early gold mineralisation cannot be ruled out. Ore textures in the Mylonite-style and Porphyry-style lodes are indicative of high-strain ductile deformation e.g. grainsize reduction (mylonitic texture) due to intense ductile shear deformation (Lister and Snoke, 1984; Davis and Reynolds, 1996) in the Mylonite-style lodes, and a well-developed S-C fabric in the Porphyry-style lodes.

Hydrothermal alteration associated with Mylonite-Style gold mineralisation is progressive with biotite and sericite overprinted by ankerite. Magnetite is in disequilibrium with gold-bearing fluids and is replaced by pyrite with increasing proximity to the ore zone. Porphyry-Style alteration is also progressive with an early stage of hydrothermal albite alteration overprinted by biotite and pyrite, both of which are in textural equilibrium with gold and tellurides. Gold and gold-bearing tellurides are present in both mineralisation styles as inclusions hosted within disseminated pyrite which is in textural equilibrium with biotite. Pressure shadows developed at the margins of gold-bearing pyrite grains indicates that D_{3NC} deformation post-dated the emplacement of gold.

Stage 2: D_{3NC} deformation and intrusion of M_2 porphyry dykes, formation of Contact-style gold lodes

The second stage in the formation of the New Celebration gold deposits is represented by the D_{3NC} deformation event and resulted in the formation of north-northwest trending, steeply west-southwest dipping shear zones. These shear zones are represented by a penetrative S_{3NC} shear foliation, well developed S-C fabrics, moderate to steep, south-southwest plunging L_{3mNC} stretching lineations, moderate to steep, northwest plunging, L_{3iNC} intersection lineations and south-southwest plunging L_{3sNC} slickenline lineations (Figure 14). Microscale kinematic indicators (e.g. the relationship between S- and C-foliation planes, the shape of sigmoidal quartz grains and the orientation of L_{3mNC} mineral elongation lineations) indicate that sinistral oblique-slip, west-block-down movement towards the south-southwest prevailed during D_{3NC} deformation.

Stage II magmatism, coeval with D_{3NC} deformation, resulted in the intrusion of M_2 quartz-feldspar porphyry dykes along the sheared mafic-ultramafic rock contact. Oblique-slip deformation during the D_{3NC} deformation event has resulted in the boudinage of M_2 porphyry dykes both along strike and at depth. While the intrusion of M_2 porphyry dykes occurred possibly during the same deformation event as the intrusion of M_1 porphyry dykes, several features suggest that the M_2 dykes intruded much later in the D_{3NC} deformation event. In contrast to the M_1 porphyry dykes, the S_{3NC} foliation is not developed within M_2 porphyry dykes. Rather, the S_{3NC} foliation developed in the mafic hangingwall rocks and ultramafic footwall rocks wraps around the margins of the M_2 porphyry dykes. Relict igneous minerals and textures are also well preserved in M_2 porphyry dykes and, relative to M_1 porphyry dykes, have undergone little hydrothermal alteration. The margins of phenocrysts in M_2 porphyry dykes also show no evidence for recrystallisation (Figure 8B) as observed in the earlier porphyry dykes.

Gold mineralisation occurring coincident with D_{3NC} deformation and intrusion of M_2 porphyry dykes is represented by Contact-Style lodes hosted within high-magnesium basalt adjacent to the intrusive contact with the main M_2 quartz-feldspar porphyry dyke. Structurally, gold-bearing pyrite grains are located within S_{3NC} foliation planes parallel to the intrusive porphyry contact. Despite the similar structural setting to the Mylonite-Style and Porphyry-Style, Contact-Style lodes differ in the hydrothermal alteration assemblage associated with mineralised intervals. Hydrothermal alteration associated with Contact-Style mineralisation shows a strong lateral zonation with increasing distance from the M_2 porphyry dyke contact. The distal alteration zone is characterised by the equilibrium assemblage ankerite-biotite-chlorite with accessory magnetite and pyrite. Magnetite is variably replaced by pyrite and is interpreted to represent the early stages of progressive hydrothermal alteration. The intermediate alteration zone is marked by the disappearance of chlorite although magnetite is still present, while the proximal alteration zone is defined by ankerite-sericite-pyrite with accessory galena, pyrrhotite, hematite, rutile and gold; magnetite is not present. In contrast to the early styles of gold mineralisation, Contact-style gold lodes are not associated with biotite in the proximal alteration assemblage and tellurides have not been observed in the ore mineral assemblage.

Stage 3: D_{4NC} deformation and formation of Fracture-style gold lodes

The D_{3NC} structures were subsequently overprinted by D_{4NC} deformation represented by a widely spaced, north-northeast trending, west-northwest dipping S_{4NC} foliation developed in mafic and ultramafic host rocks, S_{4NC}-parallel V_{4NC} quartz-carbonate veins and north-northeast trending, west-northwest dipping

vein-filled faults (Figure 14). Sub-horizontal slickenline lineations associated with these faults indicate that the dominant movement on the faults was strike-slip. Due to the lack of kinematic indicators, e.g. offset on marker horizons, the sense-of-movement on D_{4NC} structures could not be determined. Fractures developed at millimetre to centimetre scale within the M_2 porphyry dykes and microscopic en echelon fractures within feldspar phenocrysts (Figure 8D) reflect a more brittle deformation style and possibly formed in response to D_{4NC} deformation.

Late gold mineralisation, represented by Fracture-Style gold lodes, occurred within a brittle deformation regime. Fracture-Style gold mineralisation is hosted within fractures developed at the margins of M_2 porphyry dykes, the timing of which is, at present, equivocal: (1) fractures formed synchronous with D_{3NC} deformation that produced the large-scale boudinage of M_2 porphyry dykes, in which case fractures would represent the brittle expression of late-D_{3NC} deformation in a competent lithology, or (2) fractures formed in response to a later brittle deformation event, possibly D_{4NC} deformation.

Hydrothermal alteration of the M_2 quartz-feldspar porphyry hosting 'Fracture' style gold mineralisation is progressive. Early alteration predating gold mineralisation is defined by the variable sericitisation and saussuritisation of igneous plagioclase phenocrysts. Sericitisation of plagioclase is pervasive throughout the porphyry host rock, the intensity of which is independent to the proximity to gold-bearing fractures. Gold is hosted within subhedral to euhedral pyrite located within fractures and is in equilibrium with ankerite and sericite; tellurides are characteristically absent from the ore mineral assemblage.

Stage 4: Post-mineralisation D_{4NC+n} deformation and hydrothermal alteration

West-dipping curviplanar faults cross-cut D_{3NC} structures and are interpreted as D_{4+nNC} structures based on the different orientation of these faults compared to D_{4NC} structures. Hydrothermal alteration was not observed associated with these faults.

Several hydrothermal alteration events occurred subsequent to the gold mineralisation events and post-dating the deformation events described above. Coarse-grained (<7mm length), decussate actinolite is developed within the ultramafic footwall rocks and has a strong affinity to the margins of M_2 porphyry dykes. Actinolite prisms cross cut the S_{3NC} foliation and show no preferred orientation. Coarse-grained, disseminated, euhedral carbonate cross-cuts the S_{3NC} foliation in both mafic and ultramafic rocks and post-dates the development of late-stage actinolite. Late-stage magnetite occurs as fine-grained, disseminated euhedral crystals which are commonly zoned with chromium-rich cores and aluminium-rich rims. Late-stage magnetite cross-cuts foliation and occurred subsequent to the actinolite and carbonate alteration events.

DISCUSSION

This structural and hydrothermal alteration analysis has highlighted several points that warrant further discussion. Firstly, the timing of the two magmatic events is crucial to establish the timing of gold mineralisation. Cross cutting relationships indicate M_1 porphyry dykes intruded prior to M_2 dykes; in addition, the internal textures of M_1 and M_2 porphyry dykes suggest very different deformation conditions. The M_1 porphyry dykes have undergone intense non-coaxial ductile deformation and hydrothermal alteration and are

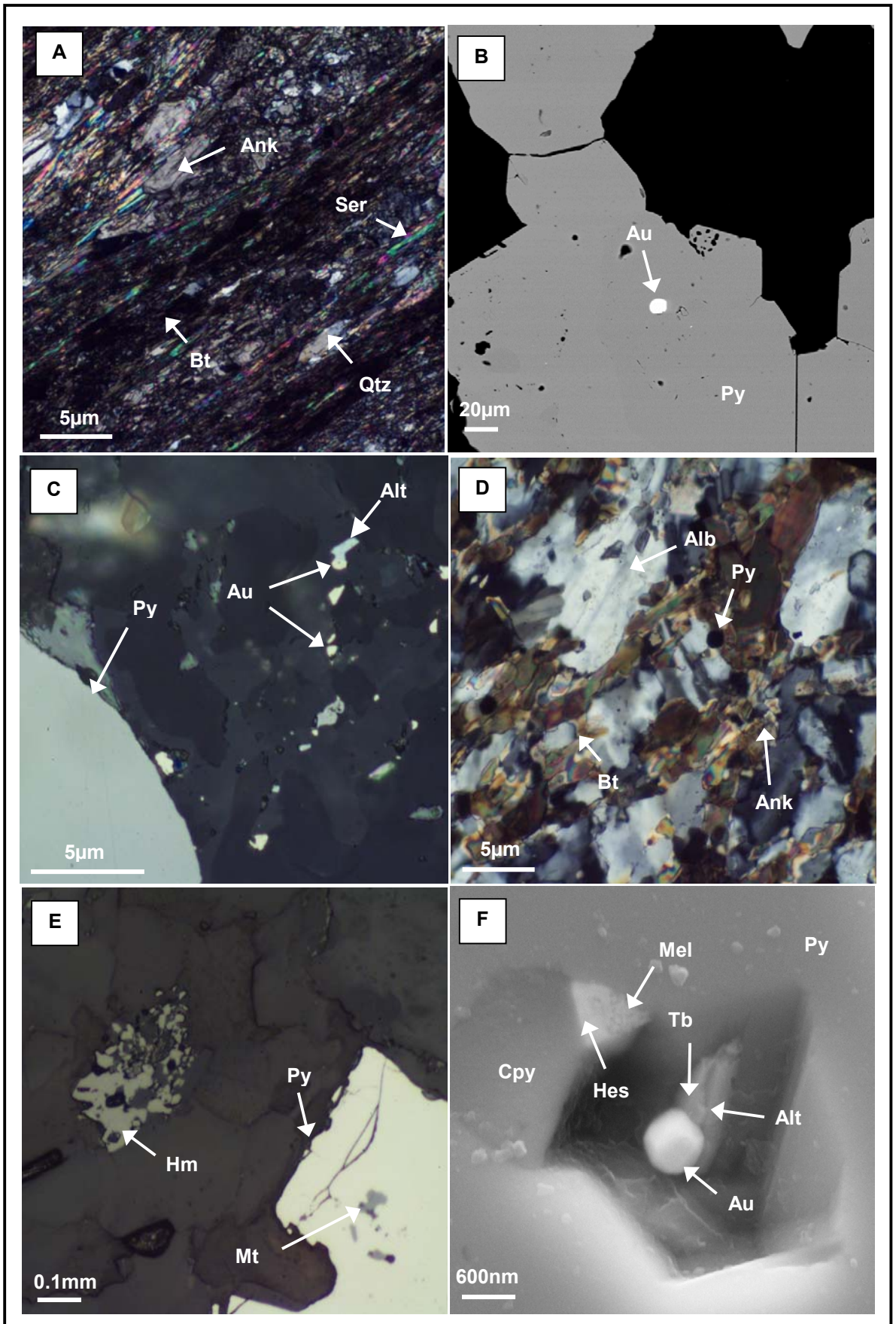

Abbreviations: Alt – Altaite; Ank – Ankerite; Au – Gold; Bt - Biotite; Cpy – Chalcopyrite; Hes – Hessite; Hm – Haematite; Mel – Melonite; Mt - Magnetite;Tb - Telurobismuth
Py – Pyrite; Qtz – Quartz; Ser – Sericite

Figure 10: Photomicrographs illustrating the hydrothermal alteration and ore petrology characteristic of Mylonite-Style (A-C) and Porphyry-Style (D-F) gold mineralisation:

A. Equilibrium mineral assemblage biotite-sericite-ankerite defining the distal alteration zone. Biotite and sericite form fine-grained elongate laths and define the well developed S_{3NC} foliation (x10 magnification).
B. Gold in the proximal alteration forms small (1 - 2µm) rounded inclusions within disseminated anhedral pyrite (x962 magnification).
C. Gold grains disseminated in silicate gangue adjacent to anhedral pyrite and in equilibrium with the lead telluride altaite (PbTe) (x40 magnification).
D. Equilibrium alteration assemblage albite-ankerite-biotite-pyrite characteristic of the ore zone of 'Porphyry' style gold mineralisation. Albite forms medium-grained, anhedral interstitial crystals with tapered, diffuse multiple twins, whereas biotite occurs as anastomosing bands of fine-grained anhedral flakes. Fine-grained ankerite forms aggregates overprinted by disseminated anhedral to euhedral pyrite (x5 magnification).
E. Hematite observed in the proximal alteration zone has a skeletal appearance and forms anhedral grains disseminated throughout the groundmass of the ore zone (x20 magnification).
F. A subhedral gold grain associated with the tellurides hessite (Hes), melonite (Mel), altaite (Alt) and tellurobismuth (Tb) contained within a cavity in pyrite (x29900 magnification).

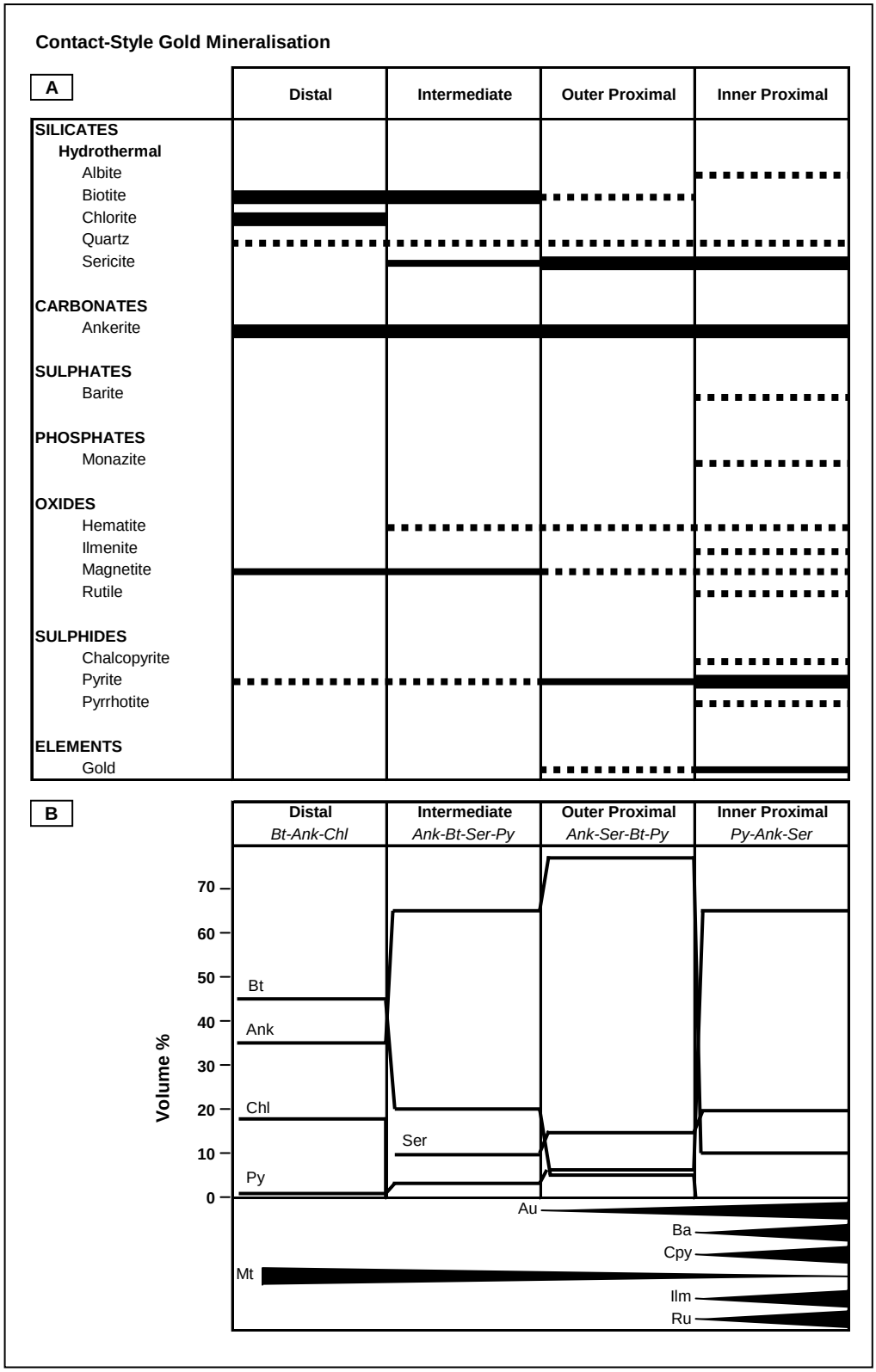

Figure 11A: Hydrothermal alteration zonation diagram illustrating changes in mineralogy across alteration zones of 'Contact-Style' mineralisation.

Figure 11B: Modal mineralogy of major and accessory minerals characteristic of the alteration zones of 'Contact-Style' mineralisation. Major minerals are displayed as volume percent.

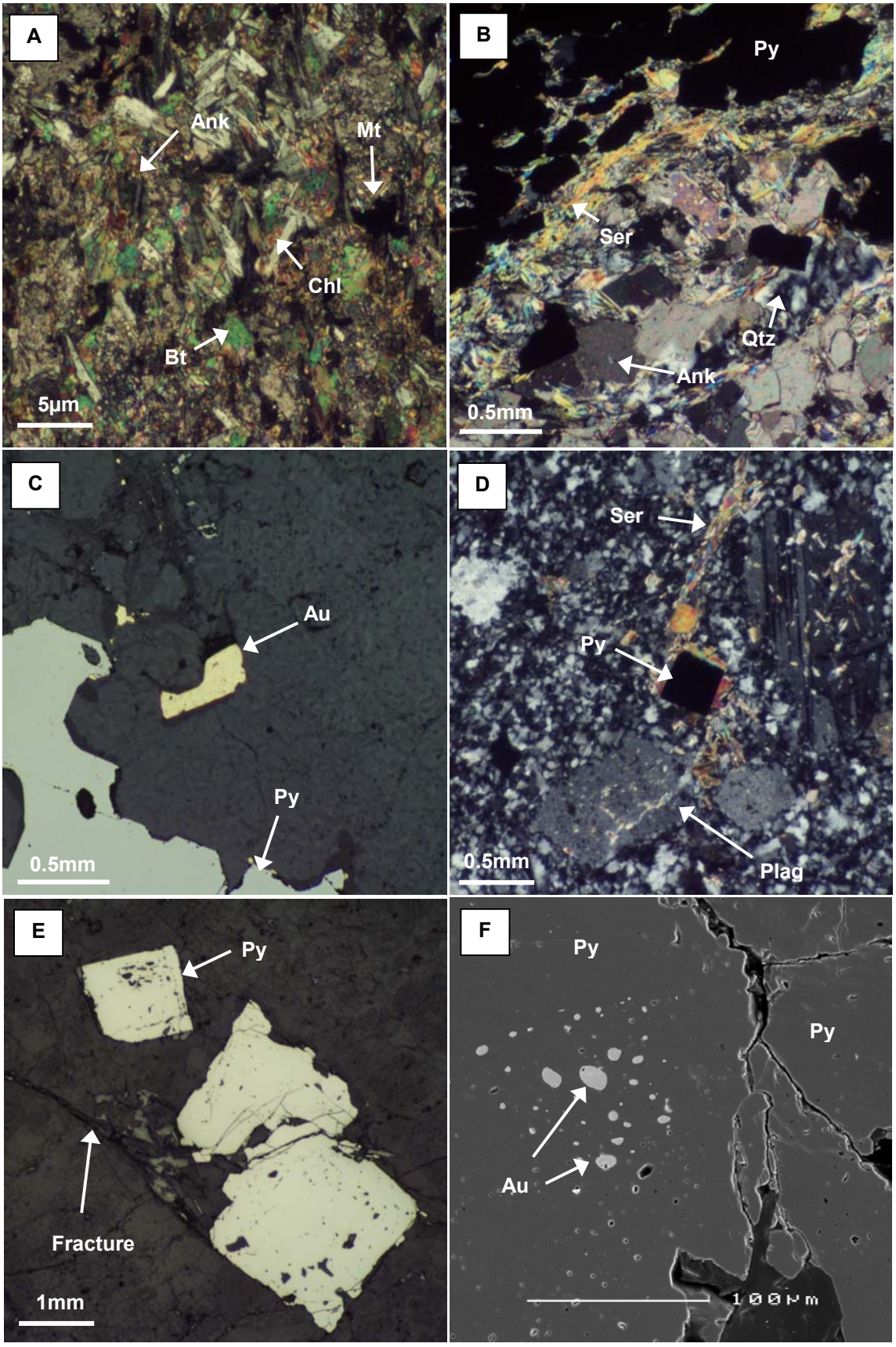

Abbreviations: Ank – Ankerite; Au – Gold; Bt - Biotite; Chl – Chlorite; Cpy – Chalcopyrite; Mt - Magnetite; Plag – Plagioclase; Py – Pyrite; Qtz – Quartz; Ser – Sericite

Figure 12: Photomicrographs illustrating the hydrothermal alteration and ore petrology of Contact-Style (A-C) and Fracture-Style (D-F) gold mineralisation:

A. Equilibrium assemblage ankerite-biotite-chlorite characteristic of the distal alteration zone. Biotite and chlorite form elongate lath shaped grains and occur in bands defining a well developed foliation. Polygranular aggregates of ankerite and disseminated anhedral magnetite overprint biotite and chlorite (x10 magnification).
B. Equilibrium alteration assemblage pyrite-sericite-ankerite characteristic of the proximal alteration zone. Sericite forms anhedral elongate flakes which wrap around pyrite aggregates, ankerite forms medium-grained anhedral crystals (x5 magnification).
C. Anhedral disseminated gold grains associated with pyrite in the inner proximal alteration zone (x20 magnification).
D. Disseminated, fine-grained, euhedral pyrite locally observed in the wall rock alteration zone (x10 magnification).
E. Pyrite in fractures forms coarse-grained euhedral crystals, commonly fractured, that contain inclusions of silicates (quartz and plagioclase) (x5 magnification).
F. Secondary electron image of small (<10µm) rounded inclusions of gold in fractured anhedral pyrite located in a fracture.

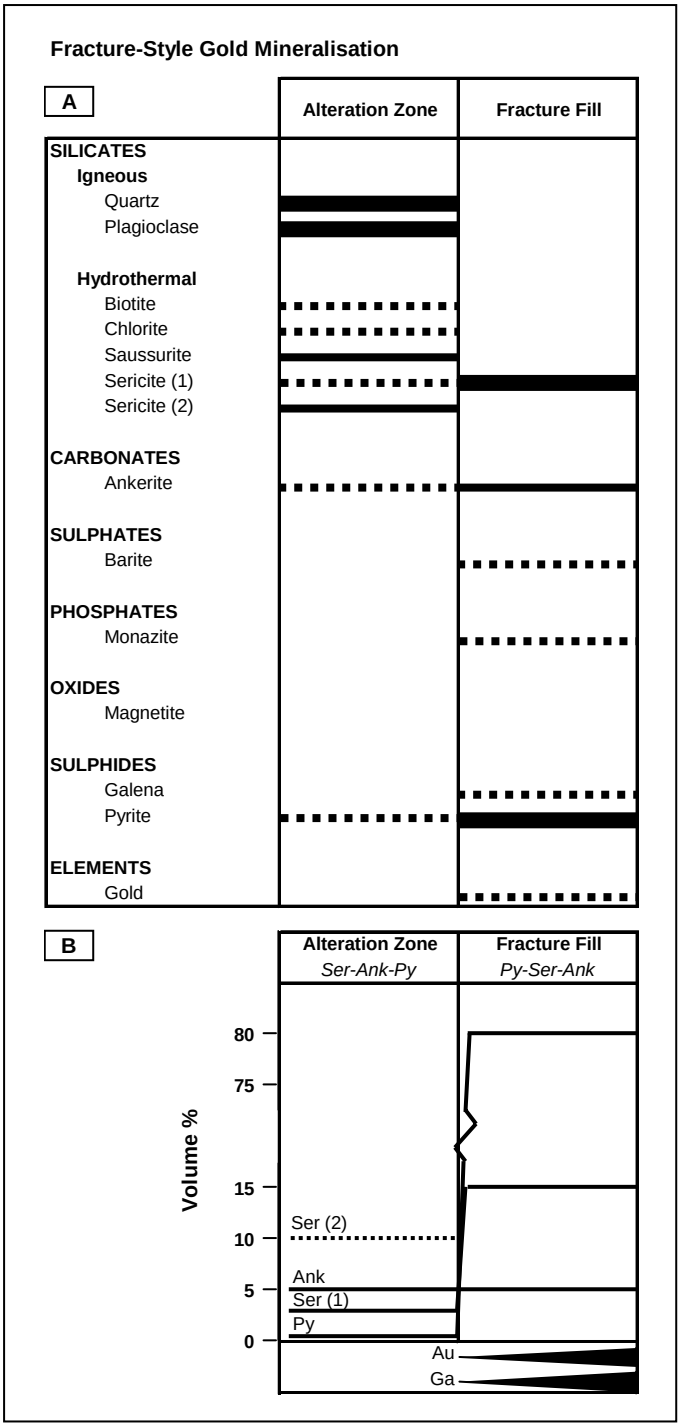

Figure 13A: Hydrothermal alteration zonation diagram illustrating changes in mineralogy across alteration zones of 'Fracture-Style' mineralisation.

Figure 13B: Modal mineralogy of major and accessory minerals characteristic of the alteration zones of 'Fracture-Style' mineralisation. Major minerals are displayed as volume percent.

A

1. D_{2NC} deformation

Tilting of stratigraphic contacts to vertical

B

2A. Early D_{3NC} sinistral, oblique-slip to the SSW, W-block down, followed by intrusion of M_1 porphyry dykes

Penetrative S_{3NC} foliation and S-C fabric developed

D_{3NC} structures developed in M_1 porphyry dykes

'Early' gold: Hosted within S_{3NC} foliation planes, associated with tellurides

Intense ductile shear strain → development of mylonites

Formation of NNW trending, WSW dipping shear zones

2B. Late D_{3NC} deformation and intrusion of M_2 porphyry dykes: boudinage of porphyry dykes – no fracturing, ductile deformation only

Boudinage of M_2 porphyry dykes

S_{3NC} foliation wrapping around porphyry boudins

Fracturing of M_2 porphyry dyke margins

Fracturing of M_2 porphyries during late-D_{3NC}

'Late' gold: Hosted within S_{3NC} foliation adjacent to M_2 porphyry dykes

C

3. Strike-slip D_{4NC} deformation

Formation of NNE trending shear zones

'Late' gold: Hosted within fractures in M_2 porphyry dykes

Boudinage of M_2 porphyry dykes

S_{3NC} foliation wrapping around M_2 porphyry dykes

N

Figure 14: Integrated structural and hydrothermal alteration model for gold mineralisation at New Celebration. ‘Early’ gold is associated with telluride species and represented by Mylonite-Style and Porphyry-Style mineralisation and introduced early during the sinistral oblique-slip D_{3NC} deformation event. ‘Late’ gold is represented by Contact-Style and Fracture-Style mineralisation. The timing of Contact-Style mineralisation, hosted within S_{3NC} foliation planes, is constrained at late-D_{3NC}, whereas the timing of Fracture-Style gold mineralisation is constrained to late-D_{3NC} to D_{4NC} deformation, depending on the timing and mode of formation of the fractures.

interpreted to have intruded during a ductile deformation regime. Deformation in the M_2 porphyry dykes is more indicative of brittle-ductile deformation conditions and hydrothermal alteration in these dykes is relatively weak. Since the timing of the intrusions of M_1 porphyry dykes in relation to camp scale deformation events may not be unequivocally determined, i.e. D_{2NC} or early D_{3NC}, it must assumed that the D_{2NC} deformation event was a non-coaxial ductile event or that the D_{3NC} deformation event was a progressive ductile to brittle-ductile deformation event.

Secondly, determining the timing of fractures hosting gold is also central to determining the timing of the 'Late' gold mineralisation event. At present the timing of fractures in M_2 porphyry dykes is somewhat equivocal and, therefore, the timing of Fracture-Style gold cannot be constrained better than late- to post-D_{3NC}. Fractures could represent: (1) the expression of D_{3NC} deformation in a rigid, competent body, or (2) the result of D_{4NC} deformation.

Thirdly, the presence of tellurides in the ore assemblage of the early gold styles may suggest a strong magmatic component in the early gold mineralisation event. However, there is some disparity in the literature regarding the origin of tellurium in hydrothermal systems. For example, Cooke and McPhail (2001) state that tellurium is transported within the vapour phase of magmatic fluids, thus implying a magmatic source. Given the strong association of the tellurium-bearing gold styles with the M_1 and M_2 porphyry dykes, this scenario is highly probable. However, Ciobanu et al. (2003) in detailed studies of orogenic gold deposits in the Banatitic Magmatic and Metallogenetic Belt in southeastern Europe have failed to document such an association, and propose that the presence of tellurides reflects the evolution of individual hydrothermal systems rather than a large-scale basement source. To date, tellurides have not been observed associated with the later gold mineralisation styles, therefore, a change in the hydrothermal fluid source from 'Early' tellurium-rich to 'Late' tellurium-poor is likely.

CONCLUSIONS

1. The structural architecture of the New Celebration gold deposits comprises four main deformation events: 1) D_{2NC} resulted in the tilting of conformable strata to near vertical orientations, 2) the D_{3NC} deformation event is defined by a penetrative north-northwest trending, steeply west-southwest dipping S_{3NC} foliation, moderate to steep south-southeast to south-southwest plunging L_{3mNC} elongation lineations, moderate to steep northwest plunging L_{3iNC} intersection lineations between S- and C-foliation planes and moderate south-southeast to south-southwest plunging L_{3sNC} slickenline lineations; movement on the fault during D_{3NC} is constrained as sinistral, oblique-slip, west-block-down to the south-southwest, 3) D_{4NC} deformation is defined by north-northeast trending, steeply west-dipping S_{4NC} foliation and sub-horizontal slickenlines developed on D_{4NC} faults; the movement on D4NC faults is tentatively constrained as tentatively constrained as dextral strike-slip, and 4) D_{4+nNC} structures which are poorly developed and include west-dipping curviplanar faults.
2. The formation of fractures in the M_2 quartz-feldspar porphyry is equivocal and could represent expression of late-D_{3NC} deformation in a competent lithology or D_{4NC} brittle deformation.
3. Two distinct stages of magmatism are recognised based on differences in mineralogy, deformation style and relative timing with respect to the structural elements. The M_1 plagioclase-rich porphyry dykes were emplaced into a high-strain, ductile deformation environment (possibly prior to the onset of

the D_{3NC} deformation event) and have been deformed by D_{3NC}. The M_1 porphyry dykes show evidence for recrystallistion, whereas M_2 porphyry dykes display only minor degrees of hydrothermal alteration, no evidence of recrystallisation and well preserved relict igneous minerals and textures. The S_{3NC} foliation developed in the mafic and ultramafic host rocks wraps around the M_2 porphyry dykes that have been boudinaged both at depth and along strike during sinistral, oblique-slip D_{3NC} deformation.

4. Differences in textures and styles of deformation observed in the M_1 and M_2 porphyry dykes indicate intrusion during different deformation conditions, i.e. M_1 porphyry dykes intruded during high-strain ductile conditions, whereas M_2 porphyry dykes intruded during brittle-ductile conditions. Relative timing relationships with the structural elements of each deformation event suggest intrusion of both generations of porphyry dykes during D_{3NC}, although the intrusion of M_1 porphyry dykes during D_{2NC} cannot be ruled out; based on the above mentioned differences in the porphyries, D_{3NC} deformation is interpreted to be a long-lived progressive deformation event ranging from early ductile to late brittle-ductile deformation.
5. Four styles of gold mineralisation are recognised at New Celebration: (1) Mylonite-Style is located within quartz-ankerite-biotite-sericite mylonite of the mafic hangingwall, gold is hosted within pyrite aligned parallel to the S_{3NC} foliation and associated with biotite-ankerite$\pm$pyrite$\pm$tellurides, (2) Porphyry-Style is hosted entirely within M_1 porphyry dykes which have undergone intense metasomatism and ductile deformation. Gold is associated with pyrite hosted in S_{3NC} foliation planes and is in equilibrium with biotite-ankerite and tellurides, (3) Contact-Style gold mineralisation is hosted with high-magnesium basalt adjacent to the intrusive contact with M_2 quartz-feldspar porphyry dykes and is associated with ankerite-sericite-pyrite, and 4) Fracture-Style gold mineralisation located within brittle fractures developed at the margins of boudinaged M_2 quartz-feldspar porphyry dykes.
6. Two gold events are recognised at New Celebration. 'Early' gold, represented by Mylonite-Style and Porphyry-Style mineralisation, associated with biotite-ankerite$\pm$pyrite alteration and gold-bearing (e.g. calerverite and petzite) and non-gold-bearing (e.g. altaite, melonite and hessite) tellurides and structurally located in D_{3NC} structures, i.e. the S_{3NC} foliation. Timing of this gold event is interpreted as early-D_{3NC} deformation. 'Late' gold, represented by Contact-Style and Fracture-Style mineralisation, is hosted within S_{3NC} foliation planes in high-magnesium basalt that wrap around the intrusive M_2 porphyry contact and in fracture networks developed at the margins of the M_2 porphyry dykes. Gold is associated with pyrite-ankerite-sericite but lacks tellurides. Timing of this gold event cannot be constrained further than late-D_{3NC} to syn-D_{4NC} deformation.
7. The four different mineralisation styles observed represent two stages of gold mineralisation occurring early within a ductile deformation regime, i.e. D_{2NC} or early D_{3NC}, and late within a brittle-ductile deformation regime, i.e. late D_{3NC} or D_{4NC}.

ACKNOWLEGMENTS

The findings presented in this paper are the results of a BSc. Honours project completed by S.J. Nichols and funded by Harmony South Kal Mines P.L., a subsidiary of Harmony Gold (Australia) P.L. Harmony is thanked for their permission to publish the information presented here. Special thanks are extended to the staff at South Kal Mines and the Centre for Microscopy and Microanalysis, University of Western Australia.

REFERENCES

Archibald, N.J., Bettenay, L.F., Binns, R.A., Groves, D.I. and Gunthorpe, R.J., 1978, The evolution of Archaean greenstone terrains, Eastern Goldfields Province, Western Australia: Precambrian Research, v. 6, p. 103-131.

Archibald, N.J., 1992, Jubilee gold deposit; geology, structure and mineralisation: Unpublished company report, 10p.

Bateman, R.J., Hagemann, S.G., McCuaig, T.C. and Swager, C.P., 2001, Protracted gold mineralization throughout Archaean orogenesis in the Kalgoorlie camp, Yilgarn Craton, Western Australia: structural, mineralogical and geochemical evolution: in Hagemann, S.G., Neumayr, P., and Witt, W.K., eds., World-class gold camps and deposits in the eastern Yilgarn craton Western Australia with special emphasis on the Eastern Goldfields Province: Geological Survey of Western Australia Record 2001/17, p. 63-98.

Bateman, R. and Hagemann, S.G., in press, Gold mineralisation throughout 45 million years of Archaean orogenesis: protracted flux of gold in the Golden Mile, Yilgarn Craton, Western Australia: Mineralium Deposita

Berthé, D., Choukroune, P. and Jegouzo, P., 1979, Orthogneiss, mylonite and non-coaxial deformation of granites: the example of the South Armorican Shear Zone: Journal of Structural Geology, v. 1, p. 31-42.

Binns, R.A., Gunthorpe, R.J. and Groves, D.I., 1976, Metamorphic patterns and development of greenstone belts in the Eastern Yilgarn Block, Western Australia: in Windley, B.F. (ed), The early history of the earth, Wiley, London, p. 303-313.

Burrows, M.D., 1997, Jubilee West prospect, Location 48, 1997 exploration program: Unpublished company report.

Ciobanu, C.L., Cook, N.J., Bogdanov, K., Kiss, O. and Vučković, B., 2003, Gold enrichment in deposits of the Banatitic Magmatic and Metallogenetic Belt, southeastern Europe: *in* Eliopoulous, D.G., ed., Mineral Exploration and Sustainable Development, Netherlands, Millpress, p.1153-1156.

Clark, M.E., Archibald, N.J. and Hodgson, C.J., 1986, The structural and metamorphic setting of the Victory Gold Mine, Kambalda, Western Australia: *in* MacDonald, A.J., ed., Proceedings of Gold ’86, an International Symposium on the Geology of Gold: Toronto, p. 243–254.

Clark, M.E., 1987, The geology of the Victory Gold Mine, Kambalda, Western Australia: Unpublished PhD thesis, Queens University, Ontario, Canada, 160 p.

Clark, M.E., Carmichael, D.M., Hodgson, C.J. and Fu, M., 1989, Wall-rock alteration, Victory Gold Mine, Kambalda, Western Australia: Processes and P-T-X_{CO2} conditions of metasomatism: Economic Geology Monograph 6, p. 445–459.

Clout, J.M.F., Cleghorn, J.H. and Eaton, P.C., 1990, Geology of the Kalgoorlie gold field: Australasian Institute of Mining and Metallurgy Monograph 14, p. 411-431.

Cooke, D.R., McPhail, D.C. and Bloom, M.S., 1996, Epithermal gold mineralisation, Acupan, Baguio District, Philippines: Geology, Mineralization, Alteration and The Thermochemical Environment of Ore Deposition: Economic Geology, v. 91, p. 243-272.

Cooke, D.R. and McPhail, 2001, Epithermal Au-Ag-Te mineralisation, Acupan, Baguio District, Philippines: numerical simulations of mineral deposition: Economic Geology, v. 96, p. 109-131.

Copeland, I.K., 1998, Jubilee Gold Deposit, Kambalda: *in* Berkman, D.A. and Mackenzie D.H., eds., Geology of Australian and Papua New Guinean Mineral Deposits: Melbourne, The Australasian Institute of Mining and Metallurgy, p. 219-224.

Davis, G.H. and Reynolds, S.J., 1996, Structural Geology of Rocks and Regions, New York, John Wiley and Sons, Inc., p. 760.

Deer, W.A., Howie, R.A. and Zussman, J., 1992, An introduction to the rock-forming minerals: England, Longman Scientific and Technical, 696p.

Dielemans, P., 2000, Structural controls on gold mineralisation in the Southern Ore Zone of the Hampton Boulder Deposit, New Celebration Gold Mine, Western Australia: Unpublished M.Sc. thesis, Western Australia, University of Western Australia

Eisenlohr, B.N., Groves, D.I. and Partington, G.A., 1989, Crustal scale shear zones and their significance to Archaean gold mineralisation in Western Australia: Mineralium Deposita, v. 24, p. 1-8.

Gebre-Mariam, M., Hagemann, S.G. and Groves, D.I., 1995, A classification scheme for epigenetic Archaean lode-gold deposits: Mineralium Deposita, v. 30, p. 408-410.

Goldfarb, R.J., Groves, D.I. and Gardoll, S., 2001, Orogenic gold and geologic time; a global synthesis: Ore Geology Reviews, v.18, p.1-75.

Groves, D.I., 1993, The crustal continuum model for Late-Archaean lode-gold deposits of the Yilgarn Block, Western Australia: Mineralium Deposita, v. 28, p. 366-374.

Groves, D.I., Ridley, J.R., Bloem, M.J., Gebre-Mariam, M., Hagemann, S.G., Hronsky, M.A., Knight, J.T., McNaughton, N.J., Ojala, J., Veilreicher, R.M., McCuaig, T.C. and Holyland, P.W., 1995, Lode-gold deposits of the Yilgarn block: products of Late Archaean crustal-scale overpressured hydrothermal systems: *in* Coward, M.P., and Ries, A.C., eds., Early Precambrian Processes, Geological Society Special Publication 95, p. 155-172.

Groves, D.I., Goldfarb, R.J., Gebre-Mariam, M., Hagemann, S.G. and Robert, F., 1998, Orogenic gold deposits: A proposed classification in the context of their crustal distribution and relationship to other gold deposit types: Ore Geology Revies, v. 13, p. 7-27.

Groves, D.I., Godfarb, R.J., Knox-Robinson, C.M., Ojala, J., Gardoll, S., Yun, G. and Holyland, P., 2000, Late-kinematic timing of orogenic gold deposits and significance for computer-based exploration techniques with emphasis on the Yilgarn Block, Western Australia: Ore Geology Reviews, v.17, p. 1-38.

Hagemann, S.G. and Cassidy, K.F., 2000, Archaean orogenic lode-gold deposits: Society of Economic Geology Reviews, v. 13, p. 9-68.

Hagemann, S.G. and Cassidy, K.F., 2001, World-class gold camps and deposits in the Eastern Goldfields Province, Yilgarn Craton: diversity in host rocks, structural controls and mineralisation styles: *in* Hagemann, S.G., Neumayr, P., and Witt, W.K., eds., World-Class Gold Camps and Deposits in the Eastern Yilgarn Craton Western Australia, with Special Emphasis on the Eastern Goldfields Province: Geological Survey of Western Australia, Record 2001/17, p. 7–44.

Hodgson, C.J., 1993, Mesothermal lode-gold deposits: *in* Kirkham, R.V., Sinclair, W.D., Thorpe, R.I., and Duke, J.M., eds., Mineral deposit modelling: Geologic Association of Canada Special Paper 40, p. 635-678.

Honman, C., 1916, The geology of the country to the south of Kalgoorlie including the mining centres of Golden Ridge and Feysville: Geological Survey Bulletin 66, p. 60-70.

Keele, R.A., 1987, Structural elements in the Jubilee deposit and their probable relationship to ore, Unpublished company report, 6p.

Kishida, A. and Kerrich, R., 1987, Hydrothermal alteration zoning and gold concentration at the Kerr-Addison Archaean Lode Gold Deposit, Kirkland Lake, Ontario: Economic Geology, v. 82, p. 649-690.

Krapez, B., Brown, S.J.A., Hand, J., Barley, M.E. and Cas, R.A.F., 2000, Age constraints on recycled crustal and supracrustal sources of Archaean metasedimentary sequences, Eastern Goldfields Province, Western Australia: evidence from SHRIMP zircon dating: Tectonophysics, v. 322, p. 89-133.

Langsford, N., 1989, Stratigraphy of Locations 48 and 50: 1989 Kalgoorlie Gold Workshops, 6p.

Laing, W.P., 1994, Ore systems at New Celebration and Ora Banda and a comparison with the Kalgoorlie system: Unpublished company report, 62p.

Lister, G.S. and Snoke, A.W., 1984, S-C Mylonites: Journal of Structural Geology, v. 6, p. 617-638.

McCuaig, T.C. and Kerrich, R., 1998, P-T-t deformation-fluid characteristics of lode-gold deposits: Evidence from alteration systematics: Ore Geology Reviews, v. 12, p. 381-453.

Maitland, A.G., 1919, Notes on some auriferous localities on the East Coolgardie Goldfield to the south of Kalgoorlie: Annual progress report of the Geological Survey for the year 1919, p. 3-4.

Mueller, A.G. and Harris, L.B., 1987, An application of wrench tectonic models to mineralised structures in the Golden Mile District, Kalgoorlie, Western Australia: Geology Department and University Extension, The University of Western Australia, Publication 11, p.97-107.

Nelson, D.R., 1997, Evolution of the Archaean granite-greenstone terranes of the Eastern Goldfields, Western Australia: SHRIMP U-Pb zircon constraints: Precambrian Research, v.83, p. 57-81.

Neumayr, P., Hagemann, S.G., Walshe, J. and Morrison, R.S., 2003, Camp- to deposit-scale zonation of hydrothermal alteration in the St Ives gold camp, Yilgarn Craton, Western Australia: evidence for two fluid systems?, *in* Eliopoulous, D.G., ed., Mineral Exploration and Sustainable Development, Netherlands, Millpress, p. 799–803.

Newcrest Mining Limited, 2001, Hampton Boulder Jubilee Resource Report: Unpublished internal company report, 70p.

Norris, N.D. and Maddocks, G.E., 1987, Hampton Boulder Deposit, New Celebration Gold Project, Kalgoorlie District, Western Australia: Unpublished company report, 13p.

Norris, N.D., 1990, New Celebration Gold Deposits, *in* Hughes, F.E., ed., Geology of the Mineral Deposits of Australia and Papua New Guinea: Melbourne, The Australasian Institute of Mining and Metallurgy, p. 449-454.

Phillips, G.N., Groves, D.I. and Kerrich, R., 1996, Factors in the formation of the giant Kalgoorlie gold deposit: Ore Geology Reviews, v. 10, p. 295-317.

Poulsen, K.H., Robert, R. and Dube, B., 2000, Geologic classification of Canadian gold deposits: Geological Survey of Canada, Bulletin 540, 106p.

Ridley, J. and Mengler, F., 2000, Lithological and structural controls on the form and setting of vein stockwork orebodies at the Mount Charlotte gold deposit, Kalgoorlie: Economic Geology, v. 95, p. 85-98.

Robert, F. and Brown, A.C., 1986, Archaean gold-bearing quartz veins at the Sigma Mine, Abititbi Greenstone Belt, Quebec: Part I Geologic relations and formation of the vein system: Economic Geology, v. 81, p. 578-592.

Robert, F. and Poulsen, K.H., 1997, World-class Archaean gold deposits in Canada: an overview: Australian Journal of Earth Sciences, v. 44, p. 329-351.

Smith, J.P., Spooner, E.T.C., Broughton, D.W. and Ploeger, F.R., 1990, The Kerr Addison-Chesterville Archaean gold-quartz vein system, Virginiatown: Time sequence and associated mafic 'albitite' dyke swarm: Ontario Geological Survey Miscellaneous Paper, p.175-199.

Spry, P.G., Foster, F., Truckle, J.F. and Chadwick, D.F., 1997, The mineralogy of the Golden Sunlight, gold-silver telluride deposit, Whitehall, Montana, USA: Mineralogy and Petrology, v.59, p. 143-164.

Swager, C.P., 1989, Structure of Kalgoorlie greenstones-regional deformation history and implications for structural setting of the Golden Mile deposits: Geological Survey of Western Australia Report 25, p. 59-84.

Swager, C.P., Griffin, T.J., Witt, W.K., Wyche, S., Ahmat, A.L., Hunter, W.M. and McGoldrick, P.J., 1995, Geology of the Archaean Kalgoorlie Terrane – an explanatory note: Geological Survey of Western Australia Report 48, 26p.

Swager, C.P., 1997, Tectono-stratigraphy of late Archaean greenstone terranes in the southern Eastern Goldfields, Western Australia: Precambrian Research, v. 83, p. 11-42.

Vearncombe, J.R., 1989, Structure of some gold deposits at New Celebration, Western Australia, Unpublished company report, 13p.

Vogler, W.S. and Voll, G., 1981, Deformation and metamorphism at the south-margin of the Alps, Bellinzona, Switzerland, Geologische Rundschau, v. 70, p. 1232-1261.

Voll, G., 1960, New Work on Petrofabrics, Liverpool and Manchester Geological Journal, v. 2, p. 503-567.

Weinberg, R.F., Moresi, L. and van der Borgh, P., 2003, Timing of deformation in the Norseman-Wiluna Belt, Yilgarn Craton, Western Australia: Precambrian Research, v. 120, p. 219-239.

Williams, P.R., and Currie, K.L., 1993, Character and regional implication of the sheared Archaean granite-greenstone contact near Leonora, Western Australia: Precambrian Research, v.62, 343-365.

Williams, H., 1994, The lithological setting and controls on gold mineralisation in the Southern Ore Zone of the Hampton Boulder Gold Deposit, New Celebration Mine, Western Australia: Unpublished B.Sc. (Hons) thesis, Western Australia, University of Western Australia, 66p.

Williams, T., 1991, A structural and lithological investigation of the Jubilee Gold Mine with particular attention to fault structures: Unpublished B.Sc (Hons) thesis, Western Australian School of Mines.

Winkler, H.G.F., 1979, Petrogenesis of Metamorphic Rocks, New York, Springer-Verlag, 348p.

Witt, W.K., 1991, Regional metamorphic controls on alteration associated with gold mineralization in the Eastern Goldfields Province, Western Australia; implications for the timing and origin of Archaean lode-gold deposits: Geology, v.19, p.982-985.

Witt, W.K., 1993, Gold Deposits of the Kalgoorlie-Kambalda-St Ives Areas, Western Australia: Geological Survey of Western Australia Record 1992/15, 107p.

Witt, W.K., Knight, J.T. and Mikucki, E.J., 1997, A synmetamorphic lateral fluid flow model for gold mineralization in the Archaean southern Kalgoorlie and Norseman terranes, Western Australia: Economic Geology, v. 92, p. 407-437.

Witt, W.K. and Vanderhor, F., 1998, Diversity within a unified model for Archaean gold mineralization in the Yilgarn Craton of Western Australia: An overview of the late-orogenic, structurally-controlled gold deposits: Ore Geology Reviews, v. 13, p. 29-64.

Yeats, C.J., McNaughton, N.J., Ruettger, D., Bateman, R., Groves, D.I., Harris, J.L. and Kohler, E., 1999, Evidence for diachronous Archaean lode gold mineralisation in the Yilgarn Craton, Western Australia: A SHRIMP U-Pb study of intrusive rocks: Economic Geology, v. 94, p. 1259-1276.